Detailed report on local meteorological conditions
Deliverable 6.4 iSCAPE project

iSCAPE

Detailed report on local meteorological conditions

D6.4

07/2019

This project has received funding from the European Union's Horizon 2020 research and innovation programme under grant agreement No 689954.

Project Acronym and Name	iSCAPE - Improving the Smart Control of Air Pollution in Europe	
Grant Agreement Number	689954	
Document Type	Report	
Document version & WP No.	V0.4	WP6
Document Title	Detailed report on local meteorological conditions	
Main authors	Kirsti Jylhä, Carl Fortelius, Olli Saranko, Kimmo Ruosteenoja, Silvana Di Sabatino, Erika Brattich	
Partner in charge	Finnish Meteorological Institute (FMI)	
Contributing partners	ARPA-ER, UNIBO	
Release date	8.7.2019	

Document Control Page	
Short Description	*This report documents findings from Task 6.4.1 "Simulation of Climate Change in test case EU Cities". The report includes climate projections for all iSCAPE target cities: Bologna, Bottrop, Dublin, Guilford, Hasselt and Vantaa. The magnitudes of climatic changes in the six cities by the year 2050 were derived from a large number of climate model simulations. An atmosphere-surface interaction module was then used to study climatic impacts of a "Passive Control System" (PCS) intervention in one of the cities, Vantaa, in the current climate and in a projected future climate. The intervention consisted of increasing the fraction of green spaces and relatively sparsely built suburban-type land use at the expense of more densely built commercial and industrial areas.*

Review status	Action	Person	Date
	Quality Check	*Coordination Team*	
	Internal Review	*Stefan Greiving (TUDO)* *Gopinath Kalaiarasan (UoS)*	
Distribution	Public		

Revision history			
Version	**Date**	**Modified by**	**Comments**
V0.1	13/5/2019	Kirsti Jylhä, Carl Fortelius, Olli Saranko, Kimmo Ruosteenoja, Silvana Di Sabatino, Erika Brattich	The first draft.
V0.2	5/6/2019	Kirsti Jylhä, Carl Fortelius, Olli Saranko, Kimmo Ruosteenoja, Silvana Di Sabatino, Erika Brattich	Mainly linguistic modifications.
V0.3	19/6/2019	The authors	Addressed a reviewer's (Stefan Greiving) comments
V0.4	8/7/2019	The authors	Addressed another reviewer's (Gopinath Kalaiarasan Stefan Greiving) comments

Statement of originality:

This deliverable contains original unpublished work except where clearly indicated otherwise. Acknowledgement of previously published material and of the work of others has been made through appropriate citation, quotation or both.

Table of Contents

Table of Contents

List of Tables

LIST OF FIGURES

List of abbreviations

CC:	Climate change
CMIP:	Coupled Model Intercomparison Project
CO_2:	Carbon Dioxide
D:	Deliverable
Dir:	Wind Direction
EU:	European Union
GCM:	Global Climate Model
GHG:	Greenhouse gas
IPCC:	Intergovernmental Panel on Climate Change
PCS:	Passive Control System
Prec:	Precipitation
PSL:	sea level pressure
RCP:	Representative Concentration Pathway
RCP2.6:	Low RCP in which GHG emissions are substantially reduced, leading to a radiative forcing of 2.6 W m^{-2} in the year 2100
RCP4.5:	Medium-Low RCP in which the radiative forcing is stabilized at 4.5 W m^{-2} in 2100 without ever exceeding that value
RCP6.0:	Medium-High RCP leading to a radiative forcing of 6.0 W m^{-2} in 2100.
RCP8.5:	High RCP in which GHG emissions and concentrations increase considerably over time, leading to a radiative forcing of 8.5 W m^{-2} in 2100.
Solar:	incident solar radiation at the surface
Speed	surface air wind speed
STD:	the monthly standard deviation of the temporal variability of daily mean temperature
SURFEX:	A system of physically-based numerical models of air-surface interactions
Tave:	mean surface air temperature
Tmin:	daily minimum temperature
Tmax:	daily maximum temperature
UHI:	Urban Heat Island
UNFCC:	United Nations Framework Convention on Climate Change
WMO:	World Meteorological Organization
WP:	Work Package

1 Executive Summary

The purpose of this Deliverable is to document findings from Task 6.4.1 “Simulation of Climate Change in test case EU Cities”. The task focused on climate projections for all iSCAPE target cities: Bologna in Italy, Bottrop in Germany, Dublin in Ireland, Guilford in United Kingdom, Hasselt in Belgium and Vantaa in Finland. By utilizing a large number of climate model simulations, the magnitudes of climatic changes by the year 2050 were assessed for the six cities. An atmosphere-surface interaction module was then used to study climatic impacts of a “Passive Control System” (PCS) intervention in one of the cities, Vantaa, in the current climate and in a projected future climate. The intervention consisted of increasing the fraction of green spaces and relatively sparsely built suburban-type land use at the expense of more densely built commercial and industrial areas.

The climate change assessments were grounded on simulations conducted with 28 CMIP5 global climate models. The projected changes in the climates of the iSCAPE cities were found to have several common features but also clear differences. Under a scenario of high global greenhouse gas concentrations (RCP8.5), the projected warming is expected to increase almost linearly in time during the course of the ongoing century, most rapidly in Vantaa in northern Europe and slowest in Dublin in western central Europe. Apart from Vantaa, the projected annual mean increases in daily maximum temperature are larger than those in the daily minima. The climatological (30-year average) annual mean precipitation is projected to decrease in Bologna and either increase or remain almost unaltered elsewhere. The annual total incident solar radiation is projected to increase in all six cities, most strongly in Bottrop and Hasselt and least in Vantaa and Dublin. A common feature for all the six iSCAPE cities is also that the projected changes do not distribute evenly throughout the year. However, the annual cycles of the projected changes the selected cities.

In more detail, the following changes in climate by 2050 were simulated for the test case EU cities:

- In Bologna, there is a general trend towards higher temperatures and more abundant solar radiation, particularly so in summer; in addition, the projections indicate increases in diurnal temperature range and day-to-day temperature variability during the warmer half of the year, and reductions in summer precipitation. Minor decreases in mean wind speed might occur in autumn and some turning of wind directions in summer and winter.
- The projected multi-model mean changes in temperature and precipitation in Bottrop resemble those for Bologna but are in general weaker. In contrast, in summer and autumn solar radiation is expected to increase even more strongly than in Bologna. The portion of south-westerly winds might slightly increase in winter and decrease in summer.
- Among the six iSCAPE cities, the projected long-term trend of warming is weakest in Dublin, both on annual and monthly bases. Also, the relative increase in annual insolation is lower in Dublin than in most of the other iSCAPE cities. The same is true for increases in diurnal temperature range in summer. Conversely, the projected percentage decreases in summer precipitation and increases in day-to-day variability in daily mean temperatures in summer are of the average magnitude, whereas the decreases in mean wind in summer are slightly larger (or less minor), although with high uncertainty, than in most of the other iSCAPE cities.
- The climate projections for Guilford resemble those for Dublin in several aspects, but the changes are generally larger. The percentage increase in summertime diurnal temperature range is about twice as large as in Dublin, and the annual mean solar radiation flux is

projected to increase approximately at the same rate as in Bologna, although not as rapidly as in Bottrop and Hasselt.

- The climate projections for Hasselt are very similar to those for the adjacent iSCAPE city, Bottrop. There is a general trend towards higher temperatures, particularly so in summer, slightly wetter winters and drier summers, more solar radiation and little changes in mean wind speed. The multi-model mean projections show slight increases (decreases) in the portion of south-westerly winds in winter (summer).
- The projected future changes in the climate of Vantaa in northern Europe deviate from those for the other iSCAPE cities. There is a general trend towards higher temperatures, but unlike in the other cities, the trend is stronger in winter than in summer. Also, the projected changes in precipitation and solar radiation are more pronounced in winter than in summer. In accordance with the other cities, the multi-model mean changes in the mean wind speed are small compared to the uncertainty ranges.

The test iSCAPE cities are well spread over the European latitudinal bands and represent different climate zones. The climate projections given here are well representative of the future climate change that will impact Europe and might thus be extended to other European cities.

In order to assess the impacts of the proposed passive control system (PCS), i.e. green infrastructure in this case, the air-surface interaction module SURFEX was used for the test case EU City Vantaa. The characteristics of the city-block, and the presence and properties of gardens and parks were taken into account in the simulations. The radiative and thermal properties of the building materials, as well as anthropogenic sources of heat and moisture from traffic and industry and civil buildings were likewise considered. Using specific procedures together with the CMIP5 model simulation data and the SURFEX model, future scenario weather data for Vantaa were developed at a very high temporal and spatial resolution. In these simulations, the presence of the built-up areas strongly modulates local climate, and differences between the town and the surrounding forested areas were found to remain similar to the present ones also in the 2050s.

After validation with weather observations, SURFEX was applied to explore the consequences of altering the urban layout by replacing relatively densely built commercial and industrial areas with a suburban-type land use featuring lower and less dense buildings and more widespread vegetated areas. For the city of Vantaa, this PCS intervention did not involve a dramatic change in the urban characteristics, and, accordingly the effect observed in the simulation outputs was rather modest. The strongest influence was found in wind speed

Comparing the results for the recent past climate and the mid-2050s, it was found that climate warming at street level was only slightly reduced by the simulated changes in urban morphology. By contrast, changes in morphology had an important or even dominating effect in terms of relative humidity and wind speed, compared with the projected changes in climate.

Based on urban development models considered in iSCAPE Deliverable 1.2 (‘Guidelines to promote passive methods for improving urban air quality in climate change scenarios’[1]), Vantaa can be classified as a decentralised city with no dominant core city and no clear distinction between open spaces and built-up areas. Over 60% of its area is currently green spaces and water bodies contrasting only 18% of sealed air- and watertight ground surface. The classification for Vantaa differs from that of the other iSCAPE cities, as Bologna and Dublin are examples of a compact city, and Bottrop, Guilford and Hasselt are examples of a decentralised concentration. In

[1] The report is available at the iSCAPE results webpage

addition, the current climate and the climate change projections for the city of Vantaa in northern Europe deviate from those for the other iSCAPE cities. Therefore the SURFEX model results for Vantaa, consisting of very high-resolution future scenario weather data and assessments of the PCS impacts, cannot be directly extended to the other European cities. However, the methodology could be applied for any urban areas with adequate resources.

2 Introduction

The iSCAPE project (Improving the Smart Control of Air Pollution in Europe) works on integrating and advancing the control of air quality and carbon emissions in European cities in the changing climate. iSCAPE focuses on the use of "Passive Control Systems" (PCSs) in urban spaces, on policy intervention and behavioural changes of citizens lifestyle. The target cities are Bologna in Italy, Bottrop in Germany, Dublin in Ireland, Guilford in United Kingdom, Hasselt in Belgium and Vantaa in Finland. Infrastructural PCSs in the iSCAPE cities include low boundary walls (Dublin), photocatalytic coatings (Lazzaretto in the outskirts of Bologna), urban design and planning (Bottrop) and various green infrastructures: hedge-rows (Guilford), trees (Bologna) and green urban spaces (Vantaa). For a review of the characteristics, strengths and limitations of PCSs, the reader is referred to D1.2.

WP6 of the iSCAPE project aims to quantify the impacts of the infrastructural PCSs with respect to air pollutants levels and their linkages to climate changes in the urban environment. The objective is to evaluate their effectiveness both in the current climate and under future scenarios around the year 2050. Based on a review of previous research (D1.2) as well as on the results of the current project[2], climatic and meteorological factors influence the efficiency of the PCSs at various scales. For example, the impact of trees on pollutant exposure depends, among others, on meteorological conditions (wind, turbulence) (D5.2 and D6.2). Furthermore, the air purification efficiency of photocatalytic coatings partly depends on climatic factors, such as relative humidity, solar radiation and temperature, and thereby on their changes in the future (D3.6). On the other hand, urban green and blue spaces might have a cooling effect, moderating potential overheating of cities relative to the countryside (urban heat island, UHI).

An overview of the latest understanding of climate and climate change and its connection with urban air quality was provided in iSCAPE Deliverable D1.4 (Di Sabatino et al., 2017) that also reviewed literature about the detected past and projected future climatic trends in broad iSCAPE study regions. It likewise discussed climate change modelling and downscaling approaches and presented preliminary comparisons between the iSCAPE study regions in terms of climate change projections.

[2] See the following reports that are or will be made available on the iSCAPE results webpage:
D3.6, 'Report on photocatalytic coating',
D3.8, 'Report on deployment of neighbourhood level interventions',
D5.2, 'Air pollution and meteorology monitoring report',
D5.3, 'Report on interventions',
D5.4, 'Strategic portfolio choice',
D6.2, 'Microscale CFD evaluation of PCSs impacts on air quality',
D6.3, 'Detailed report based on numerical simulations of the effect of PCS at the urban level',
D6.5, 'Detailed report of the effect of PCSs on air quality in the future CC (2050) in the target cities'.

The current report documents findings from Task 6.4.1 “Simulation of Climate Change in test case EU Cities”. The report is organized in two main parts. First, regional scale climate projections by the year 2050, derived from a large number of climate model simulations, are presented for all the six iSCAPE cities. Second, using an atmosphere-surface interaction module, climatic influences of green infrastructure are assessed for one of the cities, Vantaa in northern Europe, both in the current climate and in a projected future climate. The latter part discusses meteorological model simulations with a high temporal and spatial resolution; in principle such simulations could be conducted for any urban areas.

Previously, in D1.4 Di Sabatino et al. (2017) highlighted three different climatological variables of the highest relevance in the context of air pollutants: surface air temperature, precipitation and sea level pressure. For example, increasing temperatures and decreasing precipitation facilitate an increase in ozone due to increased biogenic emissions and photochemical rates and reduced wet removal. Changes in sea level pressure are connected with changes in wind systems, with consequences on local circulations and distribution of air masses. Here we report, for each of the six cities, climate change projections for those variables and for the following additional variables: diurnal temperature range, incident solar radiation, wind speed and wind direction. From the high-resolution simulations for Vantaa, a large number of variables were extracted. In this report, we consider a selection of them: air temperature, relative air humidity, wind speed, liquid and solid precipitation, as well as downwelling solar and thermal radiation.

The outcomes of this Task for three iSCAPE cities (Bologna, Hasselt and Vantaa) were previously utilized by WP4 to simulate the interactions of air pollution and climate change, in particular to assess the impact of behavioural changes (D4.5 ‘Report on policy options for AQ and CC’). The output of the task constitutes the basis to evaluate the effectiveness of PCSs implementation for air quality and climate change (CC) in future scenarios (ongoing D6.5).

3 Regional-scale climate projections for the iSCAPE cities

3.1 Material and methods

The development of climate change projections for the iSCAPE cities was based on processing of output from global climate models (GCMs) that participated in the latest phase of the Coupled Model Intercomparison Project, CMIP5 (Taylor et al., 2012). The next phase, CMIP6, is currently in a preparation stage (Eyring et al., 2016). The approach of using simulation data from up to 28 different models enabled us to provide reliable estimates of the inter-model spread of future climate changes in the iSCAPE cities. For a wider and more detailed discussion about climate models and methods to downscale them, see iSCAPE D1.4 (Di Sabatino et al., 2017).

3.1.1 Representative Concentration Pathways

In order to simulate future climate change, climate model experiments need assumptions about the future evolution of atmospheric composition, land use change and other driving forces of the climate system. The CMIP5 global climate models were run under the so-called Representative Concentration Pathway (RCP) scenarios for global greenhouse gases (GHGs) and aerosols (Taylor et al., 2012; van Vuuren et al., 2011). In iSCAPE, all four RCPs were applied, but the main emphasis was given to RCP8.5 and RCP4.5, illustrating high and moderate emission scenarios, respectively (Figure 1a). Due to its high concentrations and very long lifetime in the atmosphere, carbon dioxide (CO2), is the most important anthropogenic GHG. Because of its past and current human-induced emissions, together with its long residence time, the different concentration scenarios in Figure 1b almost coincide for the near future decades and start clearly diverging only after about the 2050s.

Under the RCP4.5 scenario, the global mean temperature is projected to increase by 1.4 (0.9-2.0) °C between the periods 1986-2005 and 2046-2065, while under RCP8.5 the projected global warming would be 2.0 (1.4-2.6) °C (IPCC, 2013). The global warming is not expected to stay well below 2°C above the pre-industrial level in the RCP4.5 scenario, a goal that was agreed at the 21st Conference of the Parties of the UNFCCC in Paris in 2015. Even under the RCP2.6 scenario global warming is rather likely to exceed 1.5°C.

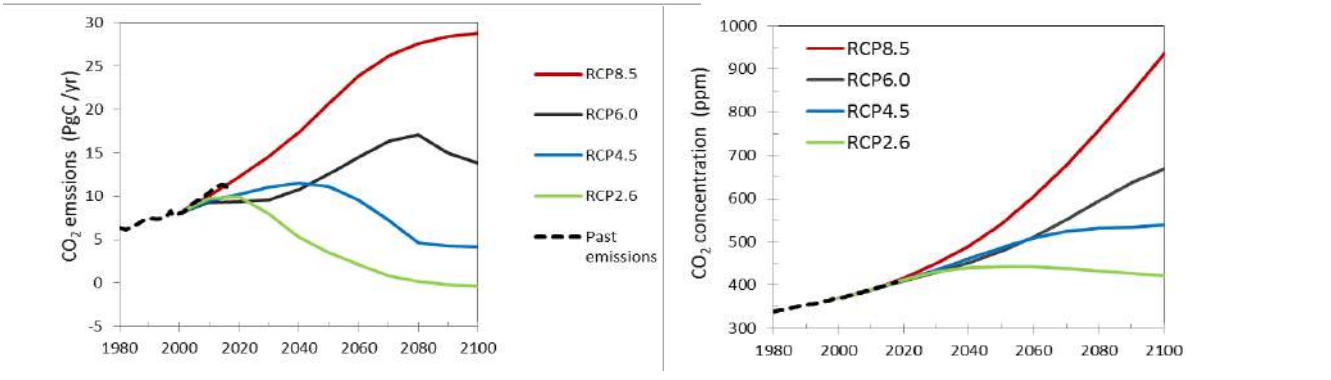

Figure 1: Temporal evolution of the global anthropogenic total emissions (left: PgC/yr) and atmospheric abundance (right: parts per million in volume) of carbon dioxide in 2000–2100 according to four RCP scenarios; see the legend (based on IPCC, 2013*). Past carbon emissions (1980-2017) from fossil fuel combustion, industrial processes and land-use changes are extracted from Global Carbon Project (2018; https://www.icos-cp.eu/GCP/2018). The observed*

abundance data are available for download from NOAA/ESRL. For the abundances of other well-mixed GHGs and aerosols, see Annex II of IPCC (2013).

3.1.2 Global climate model simulations

A large ensemble of state-of-the-art global climate model simulations, CMIP5 GCMs (Taylor et al., 2012), was utilized. The names and origins of the GCMs are provided in Table 1. The number of models used to construct the climate change projections for the iSCAPE cities was 28 for daily mean temperature, precipitation, solar radiation and air pressure, 25 for daily minimum and maximum temperature and the diurnal temperature range, 24 for wind speed, 21 for wind directions, and 22 for the monthly standard deviation of the temporal variability of daily mean temperature (Table 1). Model simulations were forced by the observational "historical" GHG concentrations up to the year 2005, after which the concentrations were adopted from the selected RCP scenarios (Figure 1).

Model	Country	Tave	Tmin, Tmax	Prec	Solar	PSL	Speed	Dir	STD
ACCESS1-0	Australia	*	*	*	*	*	*	*	*
ACCESS1-3	Australia	*	*	*	*	*	*		
BCC-CSM1-1	China	*	*	*	*	*	*	*	*
CanESM2	Canada	*	*	*	*	*	*	*	*
CMCC-CM	Italy	*	*	*	*	*	*	*	*
CMCC-CMS	Italy	*	*	*	*	*	*	*	*
CNRM-CM5	France	*	*	*	*	*	*	*	*
EC-EARTH	Europe	*	*	*	*	*	*	*	*
GFDL-CM3	USA	*	*	*	*	*	*	*	*
GFDL-ESM2M	USA	*	*	*	*	*	*	*	*
GISS-E2-H	USA	*	*	*	*	*	*		
GISS-E2-R	USA	*	*	*	*	*	*		
HadGEM2-CC	UK	*	*	*	*	*	*	*	*
HadGEM2-ES	UK	*	*	*	*	*	*	*	*
INMCM4	Russia	*	*	*	*	*	*	*	*
IPSL-CM5A-LR	France	*		*	*	*	*	*	*
IPSL-CM5A-MR	France	*		*	*	*	*	*	*
MIROC5	Japan	*	*	*	*	*	*	*	*
MIROC-ESM	Japan	*	*	*	*	*	*	*	*
MIROC-ESM-CHEM	Japan	*	*	*	*	*	*		*
MPI-ESM-LR	Germany	*	*	*	*	*	*	*	*
MPI-ESM-MR	Germany	*	*	*	*	*	*	*	*
MRI-CGCM3	Japan	*	*	*	*	*	*	*	*
NCAR-CCSM4	USA	*	*	*	*	*		*	*
NCAR-CESM1-BGC	USA	*	*	*	*	*			
NCAR-CESM1-CAM5	USA	*	*	*	*	*	*		
NorESM1-M	Norway	*	*	*	*	*		*	*
NorESM1-ME	Norway	*		*	*	*			

Table 1: CMIP5 global climate models used in creating climate change projections for the iSCAPE cities. The first and second columns give the model acronym and the country of origin; the EC-EARTH model has been developed by a

consortium of several European countries. An asterisk in columns 3–10 indicates that data from the corresponding model was utilized for a variable (Tave: mean surface air temperature; Tmin: daily minimum temperature; Tmax: daily maximum temperature; Prec: precipitation; Solar: incident solar radiation at the surface; PSL: sea level pressure; Speed: surface air wind speed; Dir: wind direction, STD: the monthly standard deviation of the temporal variability of daily mean temperature). For further information about the individual models and key references, see Table 9.A.1 of IPCC (2013).

3.1.3 Construction of the climate change projections

Here we briefly describe the methods used to post-process the model data. Since the computational grid over the globe varies among the 28 GCMs in Table 1, model data were first interpolated onto a common 0.5 x 0.5 degrees latitude-longitude grid over Europe (for the wind direction, the resolution was 2.5 degrees). For each iSCAPE city, simulated values interpolated to the position of a nearby weather station were considered.

Future trends (expressed as changes per decade) in the climate variables by the 2050s were calculated from differences between the 30-year means of the baseline-period 1981–2010 and the future period 2040-2069. As two exceptions, for the monthly standard deviation of the temporal variability of daily mean temperature and wind direction, the baseline period was 1971-2000.

As a next step, multi-model means and inter-model standard deviations for the simulated changes were computed. Following Ruosteenoja et al. (2016), the models were weighted equally, with the exception that no individual research center was given more than two votes. The multi-model means can be regarded as “best-estimates” for the future climate changes. For a fixed RCP scenario, the spread among the model projections ensues from modelling uncertainty and internal natural variability. Using the standard deviations and the normality approximation, 90% uncertainty intervals for the change were calculated. In other words, extreme scenarios (below 5th percentile and above 95th percentile) were excluded, when estimating the uncertainty ranges. However, the extreme scenarios were taken into account when calculating the multi-model means.

3.2 Results

In the following, climate change projections will be provided for climatic variables that are relevant especially for processes affecting air quality and UHI effect. The variables include daily mean, maximum and minimum temperature, diurnal temperature range, precipitation sum, incident solar radiation, sea-level air pressure, and wind speed and direction. To give an overview, we first compare the results between the six iSCAPE cities. Climate projections for each city are then considered separately in more detail.

Implications of the climate model results on the effectiveness of PCSs to improve air quality and urban thermal comfort are examined in iSCAPE Deliverable 6.5 (‘Detailed report of the effect of PCSs on air quality in the future CC (2050) in the target cities’). D6.5 considers two iSCAPE cities under present and future climate conditions, Bologna and Vantaa, as representative of different latitudinal bands impacted differently by climate change. In Bologna, the intervention consists of planting trees in a tree-free street canyon, and in Vantaa, it consists of alterations of the urban layout when substituting buildings with vegetated areas. Influences of the intervention on thermal comfort in Vantaa are also discussed in Section 4.5 of the current report.

3.2.1 Comparisons of the six iSCAPE cities

Under the RCP8.5 scenario, the projected warming increases almost linearly in time during the course of the on-going century (Figure 2a). The multi-model mean estimates (uncertainty ranges in the parenthesis) for the increase in the climatological (i.e., 30-year) annual mean temperature by the 2050s, compared to the baseline period of 1981-2010, ranges from 1.6 (0.7-2.4) °C in Dublin to 3.2 (1.2-4.4) °C in Vantaa. In the other cities except Vantaa, and in particular in Bologna, the projected warming is strongest in summer (Figure 3a). Also, the mean diurnal temperature range, i.e. the difference between monthly mean daily maximum and minimum temperatures, is projected to increase most notably there in summer and to decrease in Vantaa in winter (Figures 2b, 3b). According to the multi-model mean estimates, standard deviations of daily mean temperatures will increase in all the cities in summer, implying stronger day-to-day temperature fluctuations in the future, and vice versa in winter (Figure 3c).

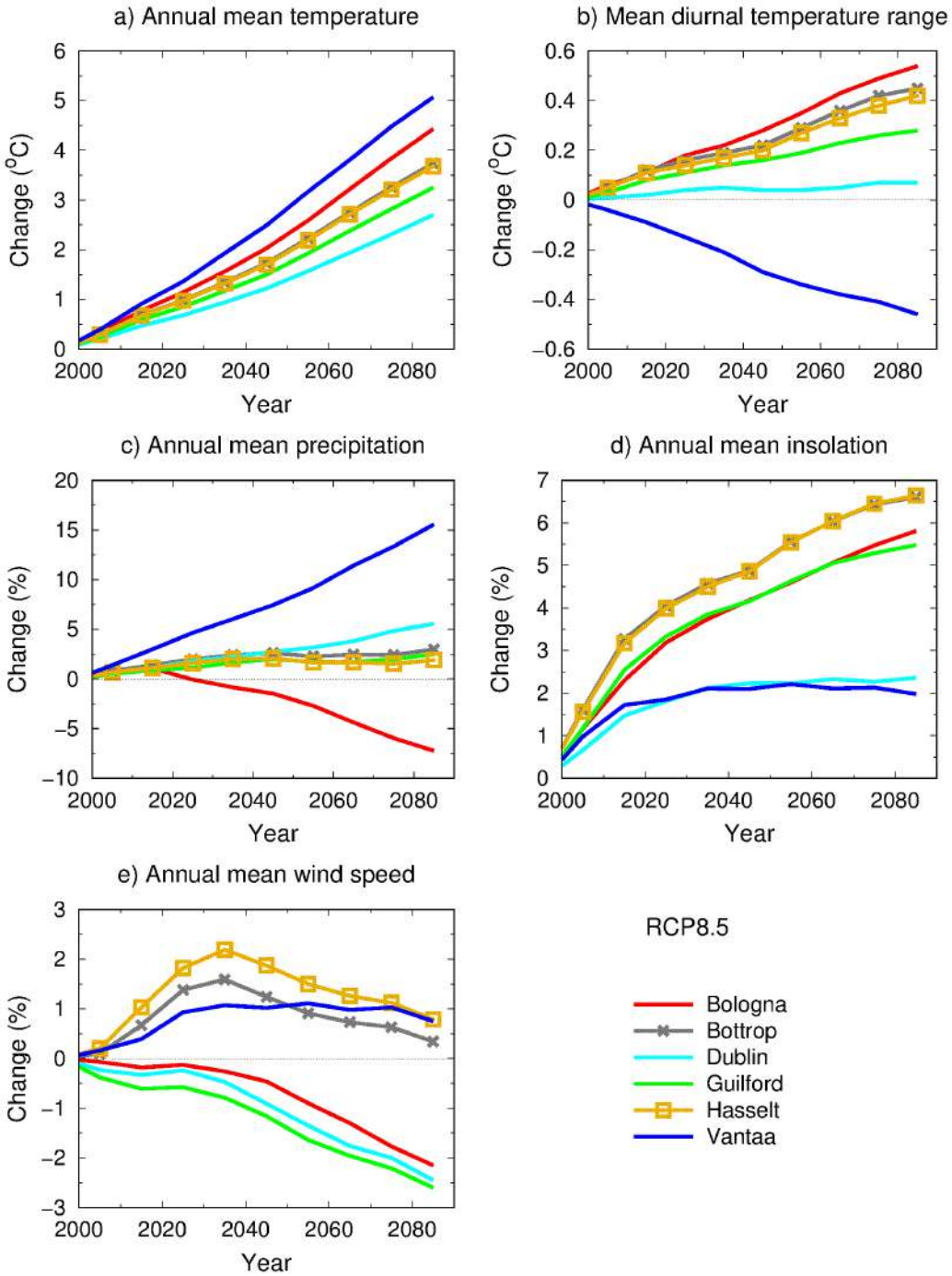

Figure 2: Projected temporal evolution of changes in 30-year averages of (a) annual mean temperature, (b) annual mean diurnal temperature range, (c) annual precipitation, (d) annual mean solar radiation flux and (e) annual mean wind speed in the six iSCAPE cities (see the legend) under the RCP8.5 scenario.

As shown in iSCAPE D1.4 and numerous previous studies (see e.g., Christensen et al., 2013; Jacob et al., 2014; Casanueva et al., 2016; Ruosteenoja et al., 2018; Lehtonen and Jylhä, 2019), the general trend is towards wetter conditions in northern Europe and drier conditions in southern Europe. Accordingly, the annual mean precipitation is projected to decrease in Bologna by -3 (-11…6) % and increase in Vantaa by 9 (1-17) % by the 2050s. In the remaining four cities, according to the multi-model mean best estimates, the annual mean precipitation would increase by a few per cents by the 2050s (Figure 2c). The changes, however, do not distribute evenly throughout the year. Even in Bologna, more wintertime precipitation can be expected in the future, while summers are likely to become drier, possibly so even in Vantaa (Figure 4a).

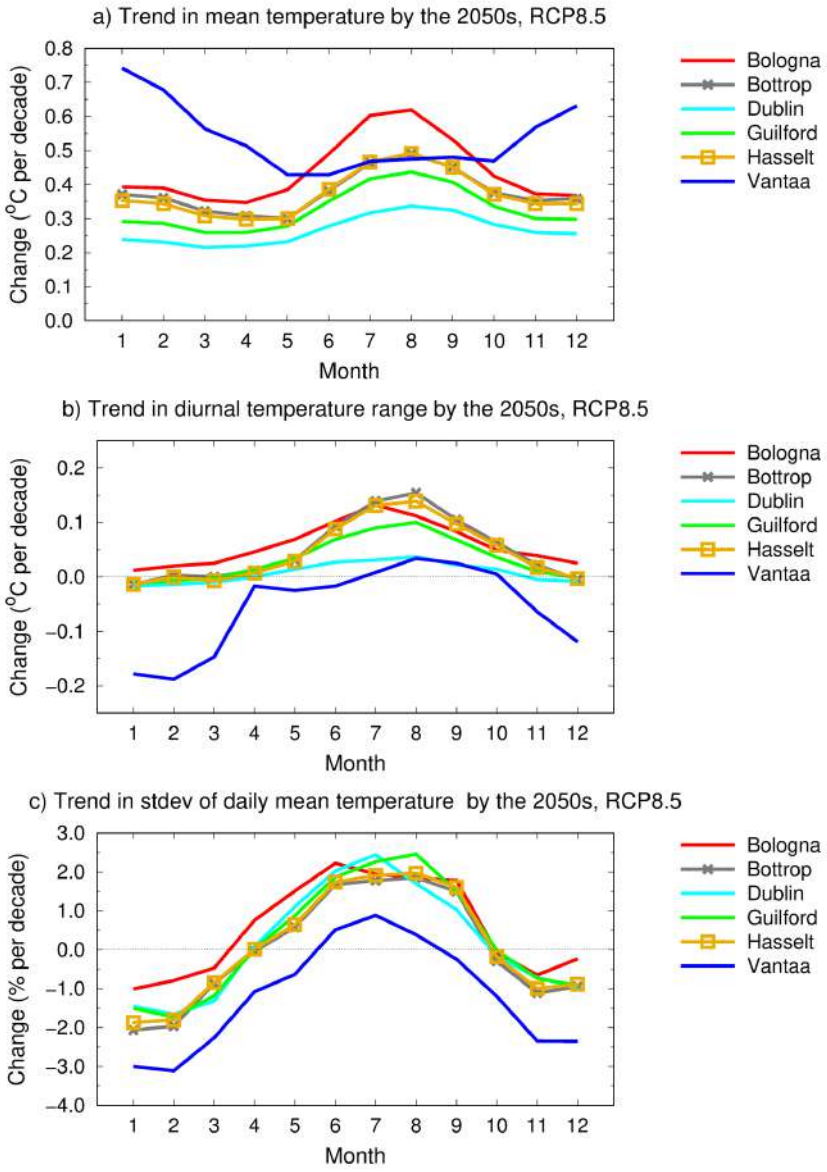

Figure 3: Projected trends in (a) monthly mean air temperature, (b) monthly mean diurnal temperature range, and (c) monthly standard deviation of the temporal variability of daily mean temperature between the baseline period and 2040-2069 in the six cities (see the legend) under the RCP8.5 scenario. The multi-model mean projections for each calendar month (1=January, 12=December) are shown. The baseline period is 1981-2010 in (a-b) and 1971-2000 in (c).

The annual total incident solar radiation is projected to increase in all six cities, most strongly in Bottrop and Hasselt, by 6 (-1…12) % and least in Vantaa and Dublin (Figure 2d). In all the cities, the projected monthly mean radiation increases are strongest in late summer and early autumn (Figure 4c). In winter, even a smaller amount of sunlight than nowadays can be expected in Vantaa and possibly also in Dublin.

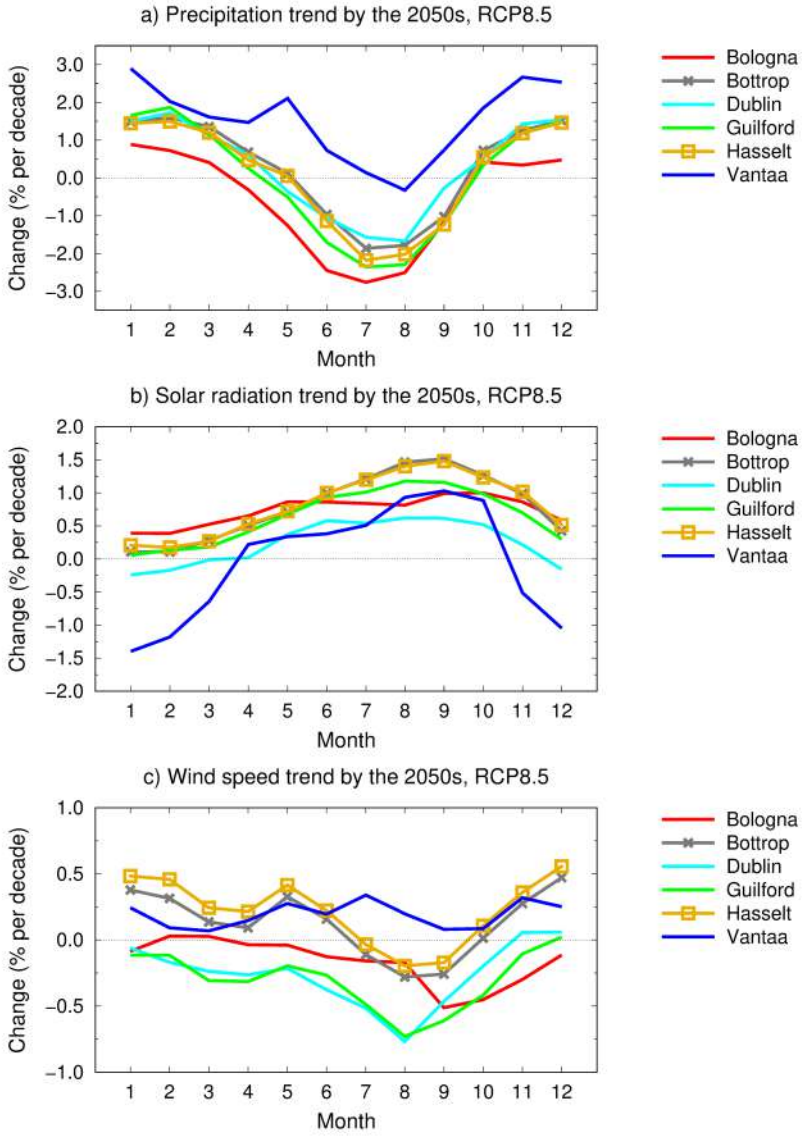

Figure 4: Projected trends in (a) monthly precipitation total, (b) monthly mean incident solar radiation, and (c) monthly mean wind speed between the periods 1981-2010 and 2040-2069 in the six cities (see the legend) under the RCP8.5 scenario. The multi-model mean projections for each calendar month (1=January, 12=December) are shown.

The decreasing precipitation totals in summer (Figure 4b) are related to strong warming in that season (Figure 3a). The lack of rain tends to decrease soil moisture, leading to reduced evapotranspiration. Thereby a larger portion of energy is transmitted into the atmosphere in the form of sensible heat. Accordingly, the joint distributions of the projected changes in summertime temperature and precipitation across the six cities, under the four RCP scenarios, indicate a clearly negative correlation between changes in the two variables (Figure 5b). Ignoring the results for Vantaa, the relation appears to be weak in winter (Figure 5a).

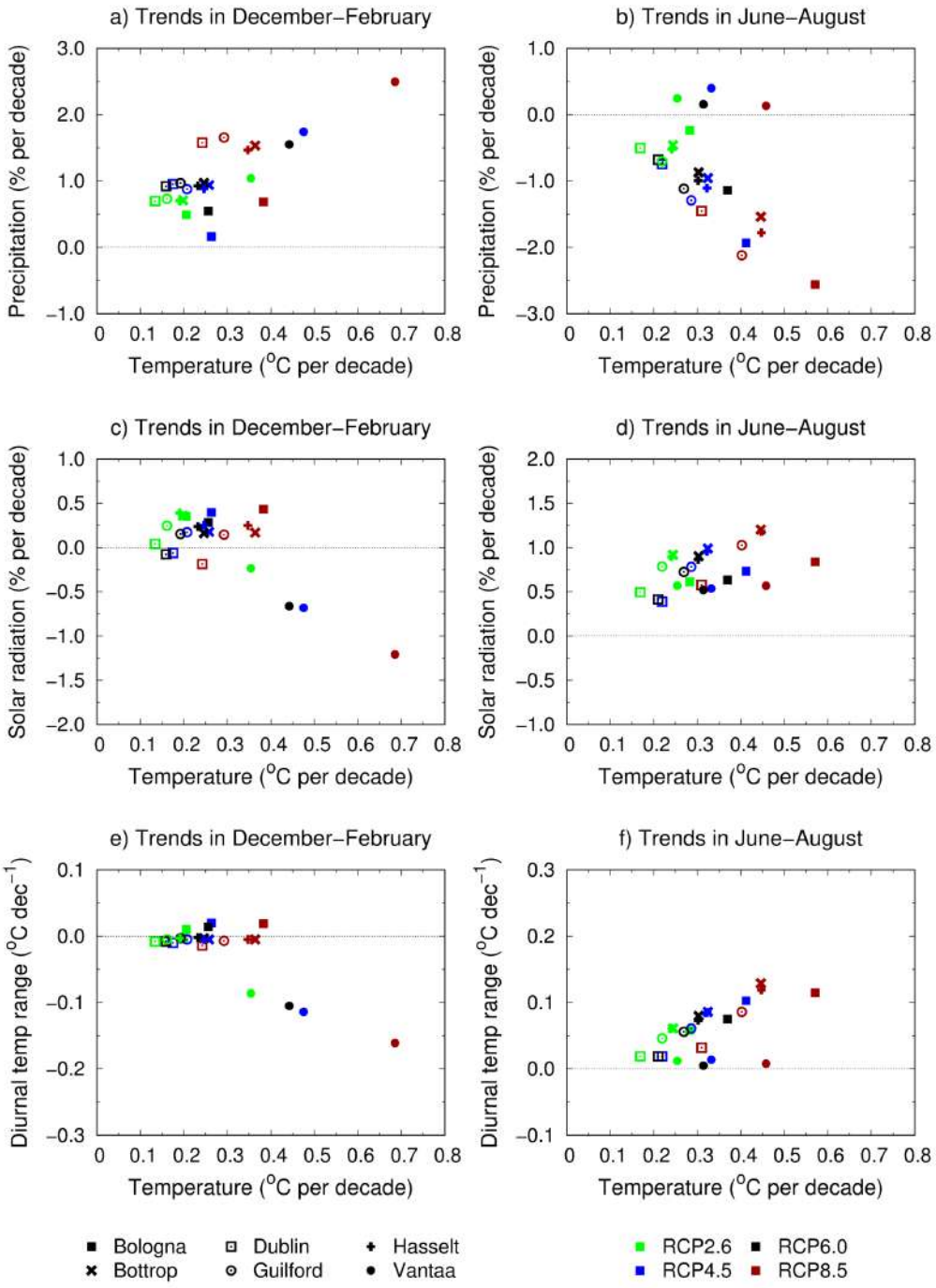

Figure 5: Scatter diagrams showing the simulated multi-model mean trends by the 2050s in temperature, in conjunction with changes in (a-b) precipitation, (c-d) incident solar radiation and (e-f) diurnal temperature range in the iSCAPE cities in winter (left) and summer (right) under four RCP greenhouse gas scenarios.

The annual cycles of the projected changes in monthly mean incident solar radiation (Figure 4c) resemble those for the diurnal temperature range (Figure 3b). Particularly in summer, the

projected increases in the two variables are strongly correlated (Figure 6b). Also the modelled summertime warming correlates positively with them (Figures 5d, 5f). The relationships are likely to be linked with changes in cloudiness in the target cities. More solar radiation due to reduced cloudiness intensifies warming particularly during the daytime, leading to strong increases in daily maximum temperatures and thereby also in the diurnal temperature range.

In winter, the joint distributions of mean temperature, precipitation, solar radiation and diurnal temperature range generally did not reveal strong inter-variable relationships (Figures 5-6). As an exception, in Vantaa at a high latitude, the projected changes in the variables under the four RCPs behaved in a physically plausible way, as discussed in more detail later (see also Ruosteenoja et al., 2016).

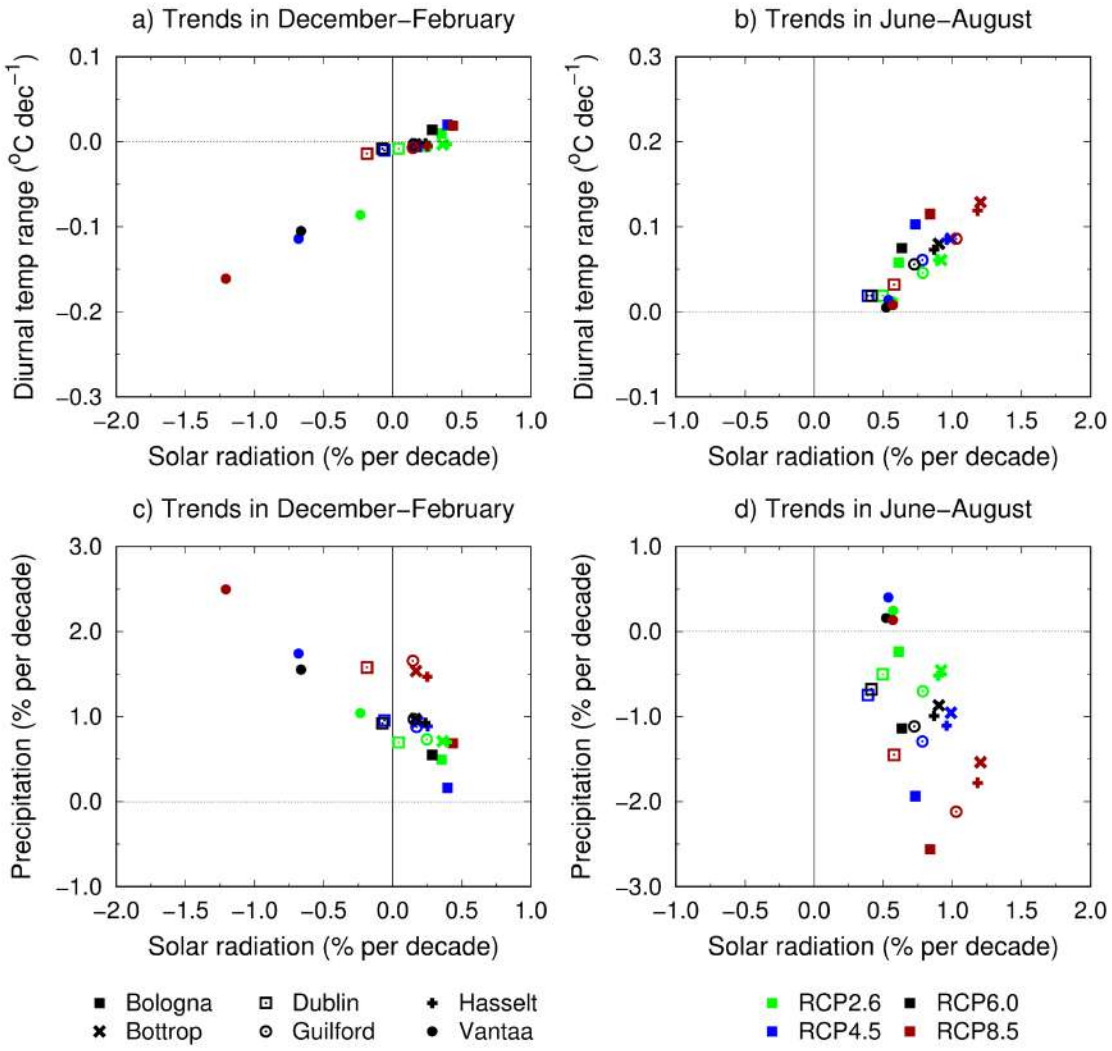

Figure 6: Scatter diagrams showing the simulated multi-model mean trends by the 2050s in incident solar radiation, in conjunction with changes in (a-b) diurnal temperature range and (c-d) precipitation in the iSCAPE cities in winter (left) and summer (right) under four RCP greenhouse gas scenarios.

According to the multi-model mean estimates, annual mean wind speed would change at most by two percent by 2050 (Figure 2e). The monthly mean wind speed would decrease at a rate of 0.8 % decade^{-1} in Dublin and Guilford in August and increase at a rate of about 0.5 % decade^{-1} in Hasselt

and Bottrop during winter months (Figure 4c). The projected changes in the other months and cities would remain between these values.

The largest changes in the frequency distributions of the simulated wind directions were found to occur in winter and summer (Figure 7). According to the multi-model mean estimates, the share of southwesterly winds would increase in winter and decrease in summer, most strongly in Hasselt (by about 3 percentage points within seven decades).

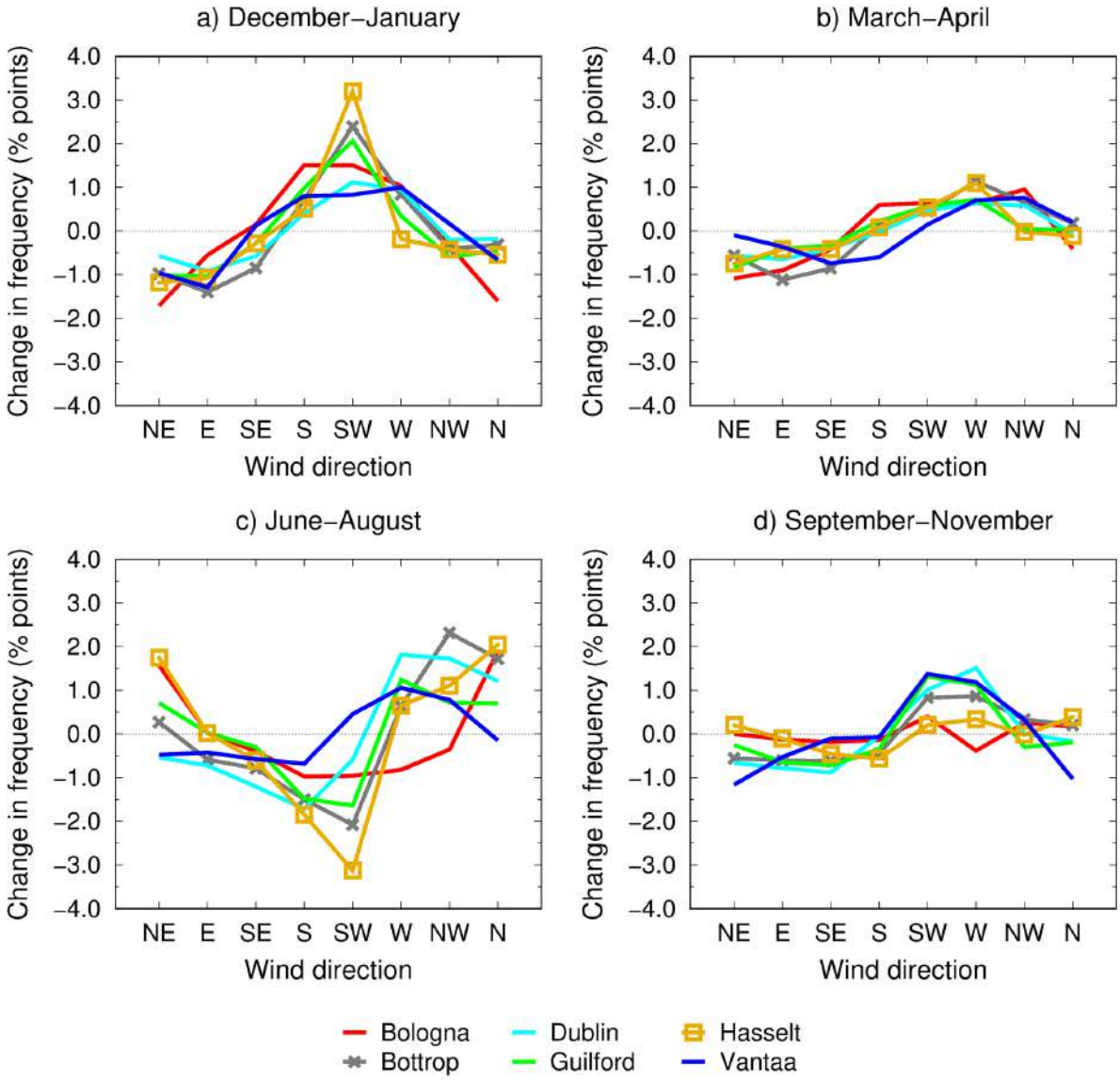

Figure 7: Projected changes in the frequency distributions of simulated wind directions in (a) winter (DJF), (b) spring (MAM), (c) summer (JJA) and (d) autumn between the periods 1971-2000 and 2040-2069 in the six cities (see the legend) under the RCP8.5 scenario. The multi-model mean projections for each cardinal and intercardinal direction are given in percentage points. To get a trend as a change in percentage points per decade, divide the values by seven.

3.2.2 Climate change projections for Bologna

In Bologna, there is a general trend towards higher temperatures and more abundant solar radiation, particularly so in summer, increases in diurnal temperature range and day-to-day temperature variability during the warmer half of the year, and reductions in summer precipitation. Minor decreases in mean wind speed might occur in autumn and some turning of wind directions in summer and winter.

In more detail, the projected warming is largest in summer and smallest in spring (Figure 8a). Under the RCP8.5 scenario, the multi-model mean seasonal estimates (the 90% uncertainty intervals in parenthesis) range from 0.36 (0.20–0.53) °C decade^{-1} in spring to 0.57 (0.28–0.86) °C decade^{-1} in summer by the 2050s. Under the RCP4.5 scenario, the projected warming rate is one third smaller.

While all the models agree on a general warming trend in all seasons, for precipitation the projected climate change signal is less clear and the spread across the models is rather wide (Figure 8b). For the summer season, the projected trend is -3 (-6…1) % decade^{-1} under RCP8.5. Winter is the only season for which the multi-model mean estimate is positive, 0.7 % decade^{-1}, the uncertainty range being -2…3 % decade^{-1}. As discussed in Section 3.2.1, the decreasing rainfall in summer contributes to the rapid warming in that season. Smaller precipitation totals result in drier soil and weaker evapotranspiration, reducing the latent heat flux and thereby increasing the share of sensible heat.

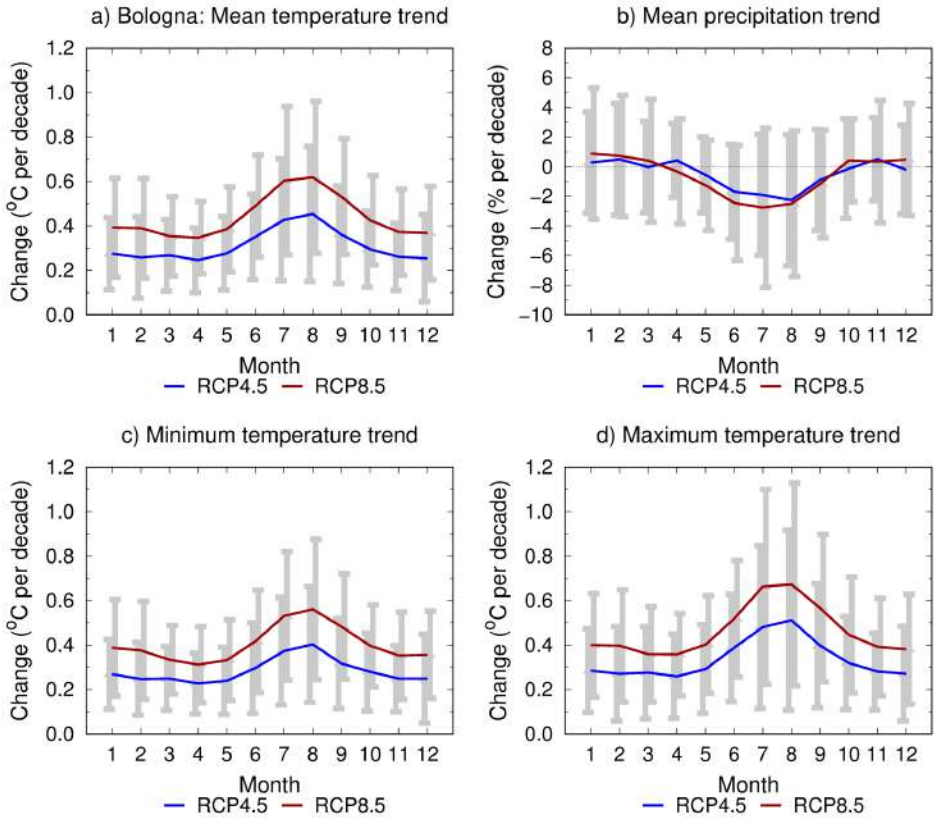

Figure 8: Projected trends in (a) monthly mean air temperature, (b) monthly precipitation total, (c) monthly mean of daily minimum temperature, and (d) monthly mean of daily maximum temperature between the periods 1981-2010 and 2040-2069 in Bologna under the RCP4.5 and RCP8.5 scenarios. The multi-model mean projections for each calendar month (1 = January, 12 = December) are depicted by solid curves (blue for RCP4.5 and red for RCP8.5). The grey bars indicate the 90 % uncertainty intervals for the change (left for RCP4.5 and right for RCP8.5).

In Bologna in winter, the projected increases in daily minimum temperatures (Figure 8c) and maximum temperatures (Figure 8d) are close to each other, and the diurnal temperature range is expected to widen only slightly (Figure 9a). In summer, daytime warming generally exceeds nocturnal warming, and the multi-model mean estimate for the seasonal mean change in the diurnal temperature range is about 0.1 °C decade^{-1}, slightly higher under the RCP8.5 than under the RCP4.5 scenario.

According to the multi-model mean estimates, the incident solar radiation will increase throughout the year, in autumn by 1.0 (-0.2…2.1) % decade^{-1} under the RCP8.5 scenario. This suggests that daytime cloudiness is likely to decrease. In summer the interpretation of diminishing cloudiness is supported by the amplification of the diurnal temperature range (Figure 9a) and reductions in precipitation amounts (Figure 8b). Based on the multi-model mean estimates, the standard deviations of daily mean temperatures will increase in summer, implying more day-to-day temperature fluctuations, and vice versa in winter (Figure 9c).

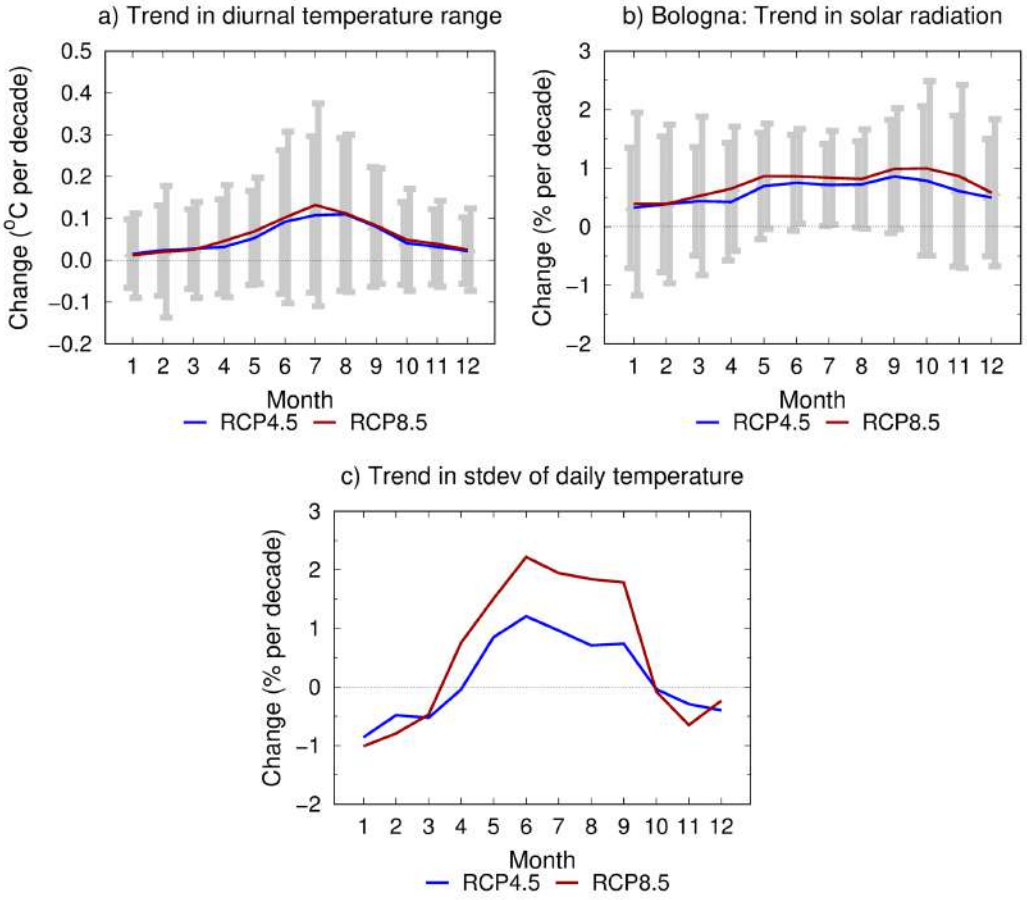

Figure 9: Projected trends in (a) monthly mean diurnal temperature range, (b) monthly mean incident solar radiation, and (c) monthly standard deviation of the temporal variability of daily mean temperature by the period 2040–2069 in Bologna under the RCP4.5 and RCP8.5 scenarios. The baseline period is 1981-2010 (top) or 1971-2000 (bottom). For further information, see the caption for Figure 8.

The multi-model mean projections show mainly slight increases in sea level air pressure in Bologna, apart from July and August (Figure 10a) and reductions in wind speed by 0.4 % decade^{-1} in autumn (Figure 10b). The inter-model differences are, however, very wide for both variables.

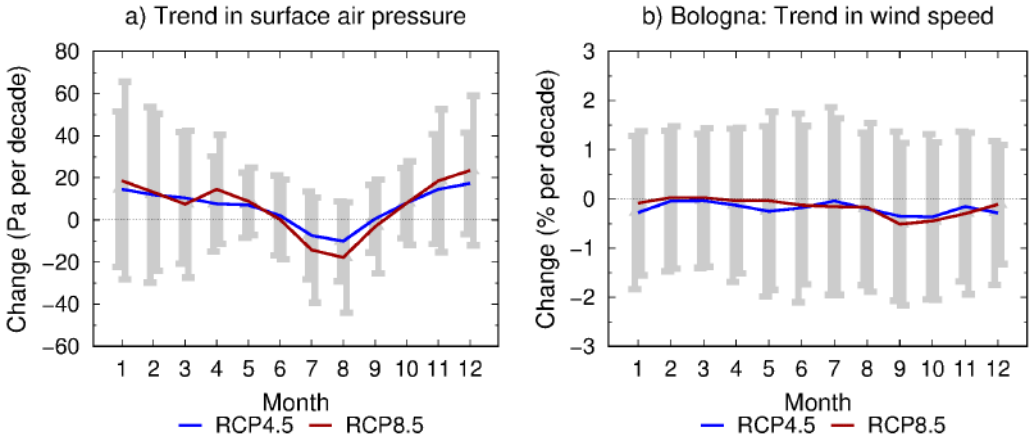

Figure 10: Projected trends in a) monthly mean surface air pressure and b) wind speed between the periods 1981-2010 and 2040-2069 in Bologna under the RCP4.5 (blue) and RCP8.5 (red) scenarios. For further information, see the caption for Figure 8.

In winter, the portions of southerly, southwesterly and westerly winds are projected to increase by 1-1.5 percentage points by the 2050s, compared to the 1980s, i.e., in seven decades (Figure 11). In summer, in contrast, the frequency of northerly and northeasterly wind would increase at the expense of southerly and westerly winds.

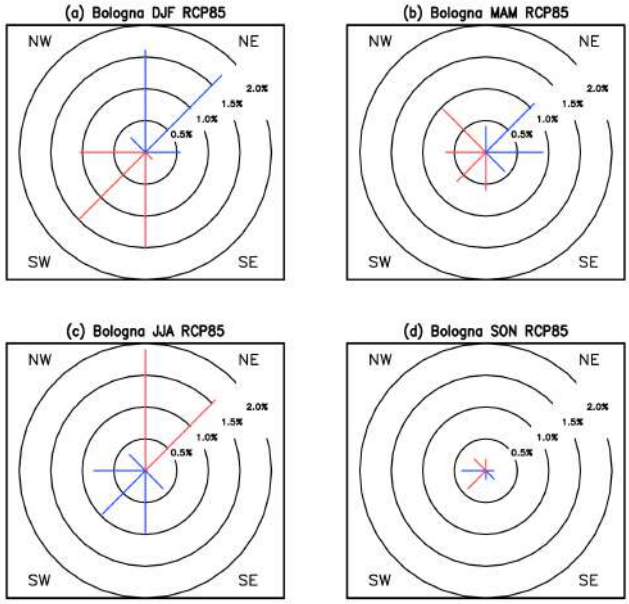

Figure 11. Projected multi-model mean changes in the frequency distributions of simulated wind directions in winter (DJF), spring (MAM), summer (JJA) and autumn between the periods 1971-2000 and 2040-2069 in Bologna under the RCP8.5 scenario. The changes are given in percentage points, with red bars depicting an increase and blue bars a decrease in the frequency. The circles indicate the scale of changes for each cardinal and intercardinal direction with an interval of 0.5%.

Implications of the projected climate changes in Bologna for the effectiveness of the green infrastructural interventions, consisting of planting trees in a tree-free street canyon, are discussed in iSCAPE Deliverable 6.5 ('Detailed report of the effect of PCSs on air quality in the future CC (2050) in the target cities').

3.2.3 Climate change projections for Bottrop

The projected multi-model mean changes in temperature and precipitation in Bottrop (resemble those for Bologna but are in general weaker (Figures 3-4). In contrast, solar radiation in summer and autumn is expected to increase even more strongly than in Bologna (Figure 4b). In winter, there might be slight increases in mean wind speeds (Figure 4c)). The portion of south-westerly winds might slightly increase in winter and decrease in south-westerly winds in summer (Figure 7).

The projected increases in monthly mean temperature range from 0.31 (0.15-0.47) °C decade^{-1} in spring to 0.45 (0.19-0.70) °C decade^{-1} in summer under the RCP8.5 scenario (Figure 12a). When considering both the best estimates and the uncertainty ranges for precipitation, it appears that in winter increases in precipitation are more likely than decreases and vice versa in summer but throughout the year even the sign of the changes is somewhat uncertain (Figure 12b).

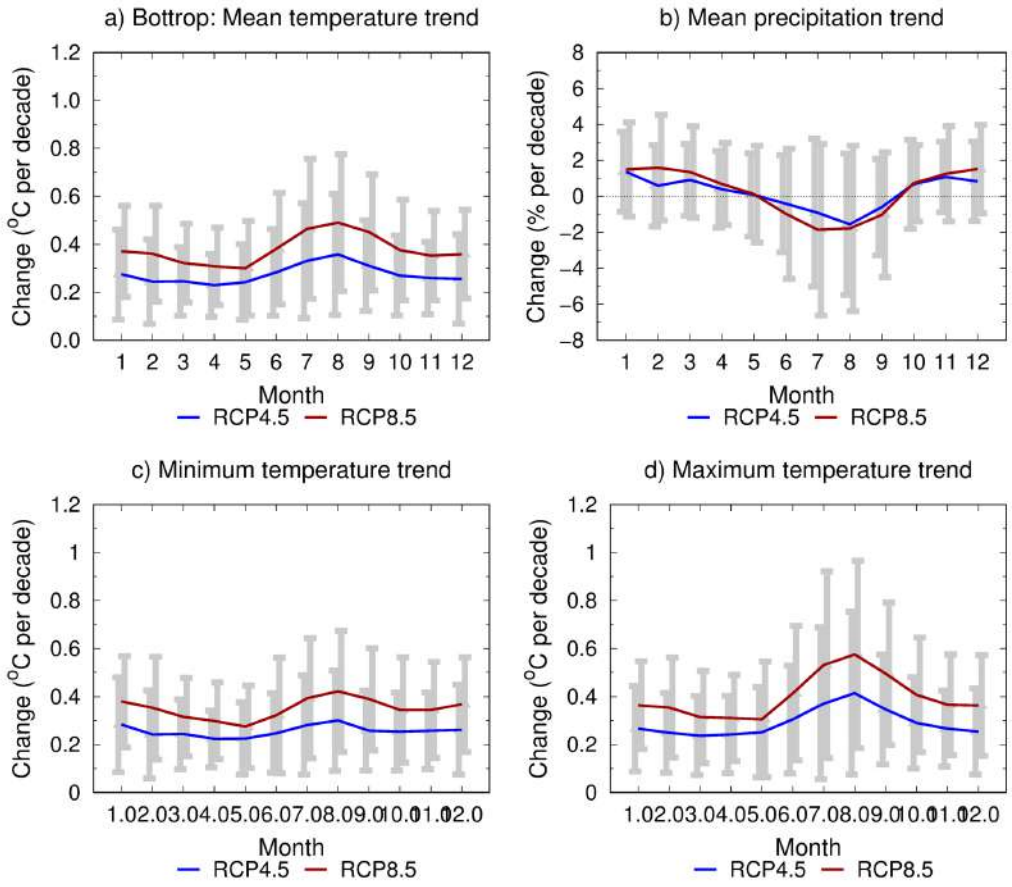

Figure 12: Projected trends in (a) monthly mean air temperature, (b) monthly precipitation total, (c) monthly mean of daily minimum temperature, and (d) monthly mean of daily maximum temperature between the periods 1981-2010 and 2040-2069 in Bottrop under the RCP4.5 and RCP8.5 scenarios. The multi-model mean projections for each calendar month (1 = January, 12 = December) are depicted by solid curves (blue for RCP4.5 and red for RCP8.5). The grey bars indicate the 90 % uncertainty intervals for the change (left for RCP4.5 and right for RCP8.5).

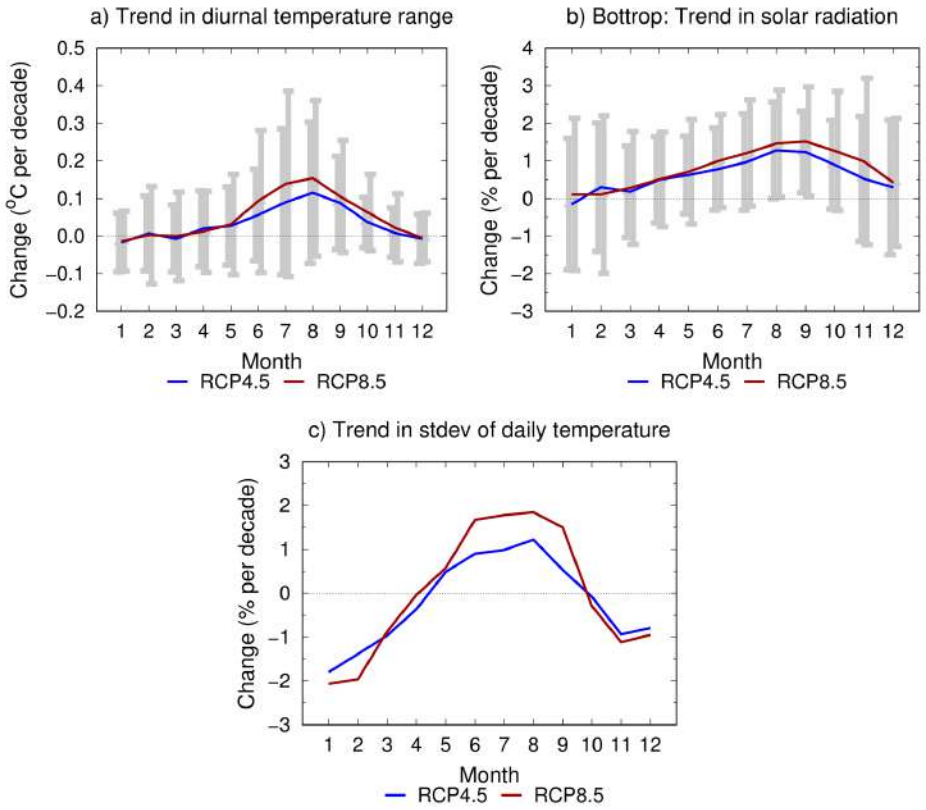

Figure 13: Projected trends in (a) monthly mean diurnal temperature range, (b) monthly mean incident solar radiation, and (c) monthly standard deviation of the temporal variability of daily mean temperature by the period 2040–2069 in Bottrop under the RCP4.5 (blue) and RCP8.5 (red) scenarios. The baseline period is 1981-2010 (top) or 1971-2000 (bottom). For further information, see the caption for Figure 12.

The increases in temperature manifest themselves as higher daily maximum temperatures in all seasons, in summer in particular, when the projected trend is 0.51 (0.18-0.84) °C decade^{-1} under RCP8.5 (Figure 12d). Since in summer the daily minimum temperatures do not increase as rapidly (Figure 12c), the seasonal mean diurnal temperature range is projected to amplify by 0.13 (-0.07...0.33) decade^{-1} (Figure 13a). In other seasons the trends for daily minimum and maximum temperatures are closer to each other and little changes in diurnal temperature range are projected to occur. On the other hand, day-to-day temperature fluctuations are projected to attenuate in winter and intensify in summer and early autumn (Figure 13c), during which time of the year incident solar radiation is also projected to increase (Figure 13b).

Based on the multi-model mean climate projections, sea level air pressure in Bottrop will slightly increase during most calendar months (Figure 14a). The inter-model differences are large for monthly mean wind speed, the multi-model mean projections suggesting small increases in winter (Figures 4c, 14b). According to Figure 15, the frequency of south-westerly winds would increase by about 2.5 percentage points in winter by the 2050s, compared to the 1980s. In summer, in

contrast, the frequency of northerly and north-westerly wind would increase at the expense of winds from the southwest.

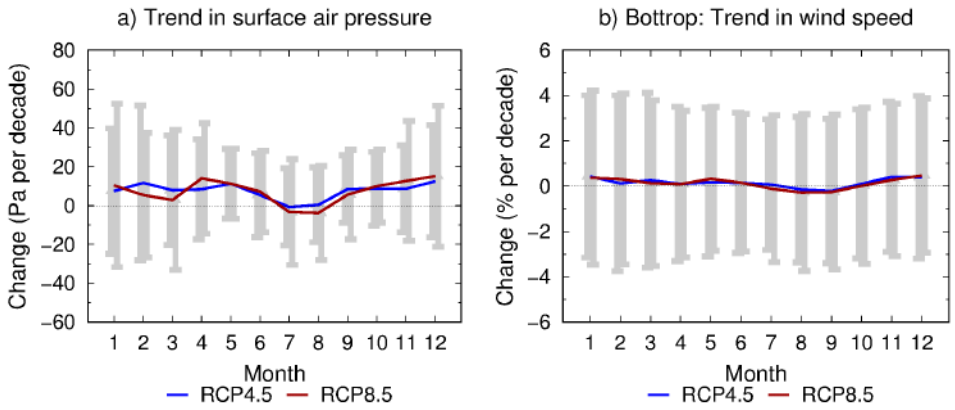

Figure 14: Projected trends in a) monthly mean surface air pressure and b) wind speed between the periods 1981-2010 and 2040-2069 in Bottrop under the RCP4.5 (blue) and RCP8.5 (red) scenarios. For further information, see caption for Figure 12.

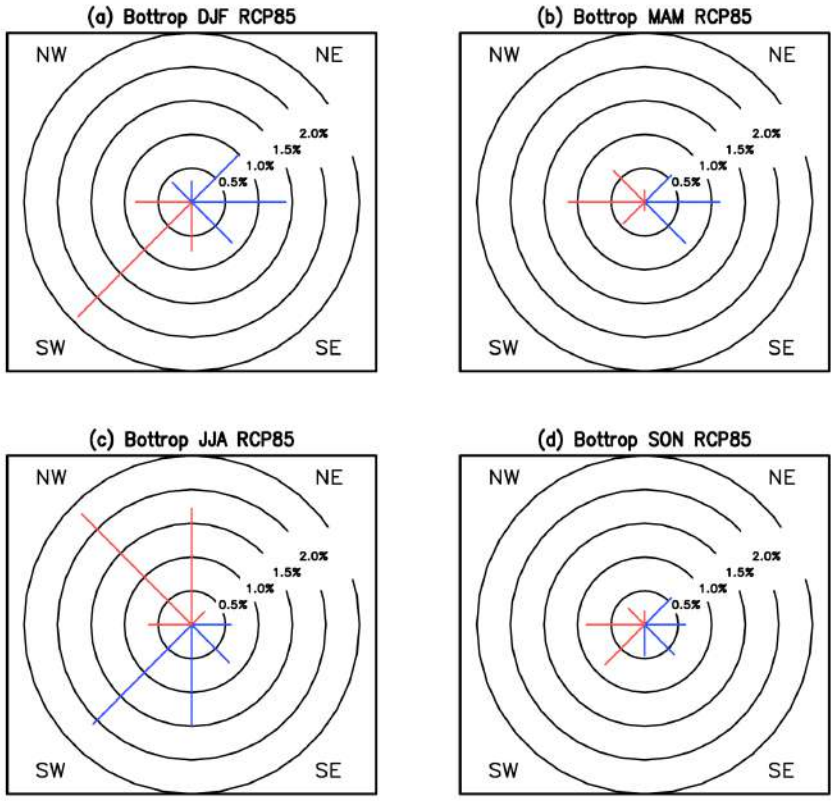

Figure 15. Projected multi-model mean changes in the frequency distributions of simulated wind directions in winter (DJF), spring (MAM), summer (JJA) and autumn between the periods 1971-2000 and 2040-2069 in Bottrop under the RCP8.5 scenario. The changes are given in percentage points, with red bars depicting an increase and blue bars a decrease in the frequency. The circles indicate the scale of changes for each cardinal and intercardinal direction with an interval of 0.5%.

3.2.4 Climate change projections for Dublin

Among the six iSCAPE cities, the projected long-term trend of warming is weakest in Dublin, both on annual and monthly basis (Figures 2-3). Also the relative increase in annual insolation is lower in Dublin than in most of the other iSCAPE cities. The same is true for increases in diurnal temperature range in summer. Instead, the projected percentage decreases in summer precipitation amounts and increases in day-to-day variability in daily mean temperatures in summer are of the average magnitude, whereas the decreases in mean wind in summer are slightly larger, although with high uncertainty, than in most of the other iSCAPE cities (Figure 4).

Analogously to the other iSCAPE cities, the projected increases in the monthly averages of daily mean, minimum and maximum temperatures in Dublin are higher under the high-emissions than under the low-emissions scenarios (Figure 16). Based on the model simulations, the seasonal mean temperature trend in summer is 0.22 (0.06–0.38) °C decade^{-1} under RCP4.5 and 0.31 (0.11–0.51) °C decade^{-1} under RCP8.5. In winter the corresponding results are 0.18 (0.07–0.28) °C decade^{-1} and 0.24 (0.13–0.35) °C decade^{-1}, respectively. Also, the monthly mean precipitation sums are projected to increase in winter and decrease in summer more strongly under RCP8.5 than under RCP4.5.

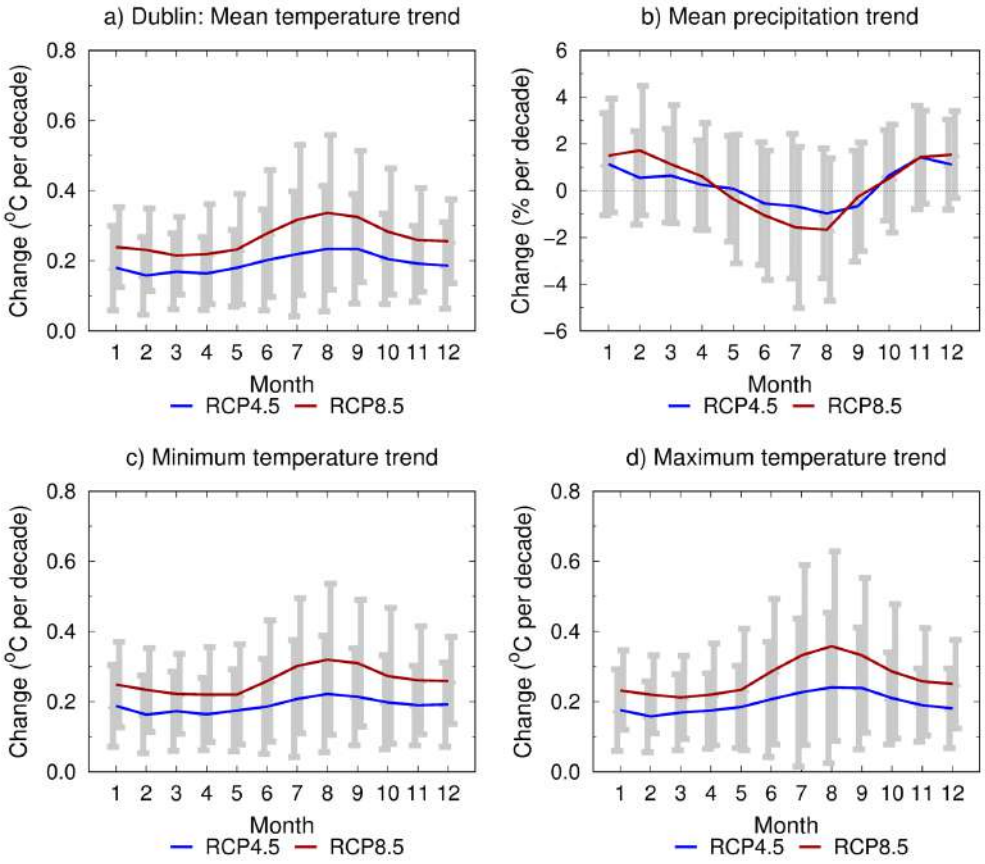

Figure 16: Projected trends in (a) monthly mean air temperature, (b) monthly precipitation total, (c) monthly mean of daily minimum temperature, and (d) monthly mean of daily maximum temperature between the periods 1981-2010 and 2040-2069 in Dublin under the RCP4.5 and RCP8.5 scenarios. The multi-model mean projections for each calendar month (1 = January, 12 = December) are depicted by solid curves (blue for RCP4.5 and red for RCP8.5). The grey bars indicate the 90 % uncertainty intervals for the change (left for RCP4.5 and right for RCP8.5).

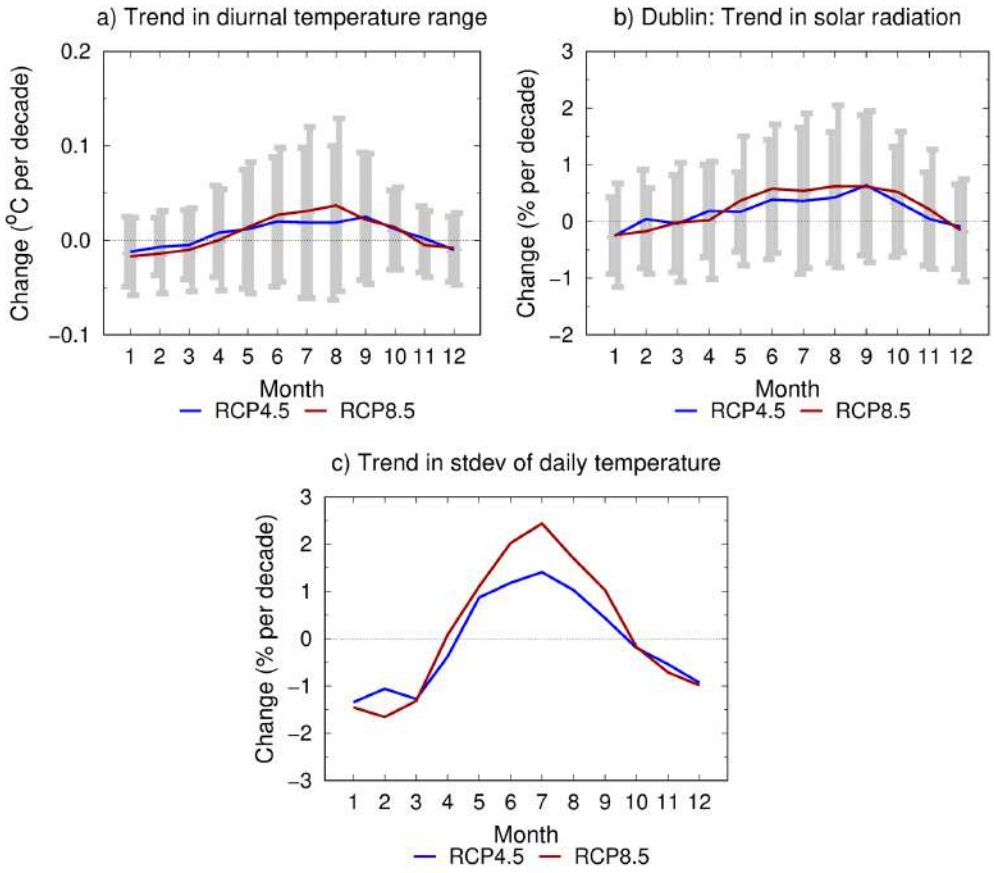

Figure 17: Projected trends in (a) monthly mean diurnal temperature range, (b) monthly mean incident solar radiation, and (c) monthly standard deviation of the temporal variability of daily mean temperature by the period 2040–2069 in Dublin under the RCP4.5 (blue) and RCP8.5 (red) scenarios. The baseline period is 1981-2010 (top) or 1971-2000 (bottom). For further information, see the caption for Figure 16.

According to the multi-model mean estimates, the monthly mean diurnal temperature ranges are projected to remain almost invariant, with minor decreases (increases) in winter (summer). The projected percentage change in summertime solar irradiance is low compared to most of the other iSCAPE cities, only 0.6 (-0.6...1.8) % decade^{-1} under the RCP8.5 scenario, whereas the increase in daily mean temperatures in summer is relatively high, about 2 % decade^{-1} (Figures 4 and 17).

The multi-model mean trend of surface air pressure is positive throughout the year, however, with high uncertainty even on the sign of the change (Figure 18a). In summer, the magnitude of mean wind is projected to change by -0.6 (-1.9…0.8) % decade^{-1} under the RCP8.5 scenario (Figure 18b) and its directional distribution is expected to shift slightly (Figure 19).

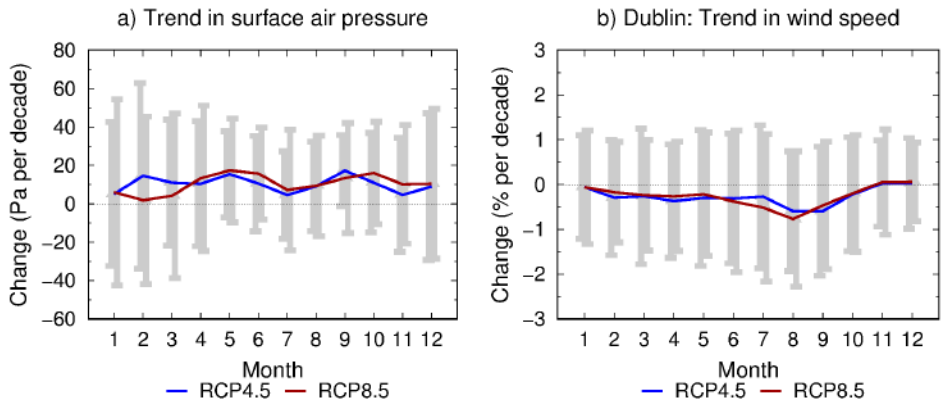

Figure 18: Projected trends in a) monthly mean surface air pressure and b) wind speed between the periods 1981-2010 and 2040-2069 in Dublin under the RCP4.5 (blue) and RCP8.5 (red) scenarios. For further information, see caption for Figure 16

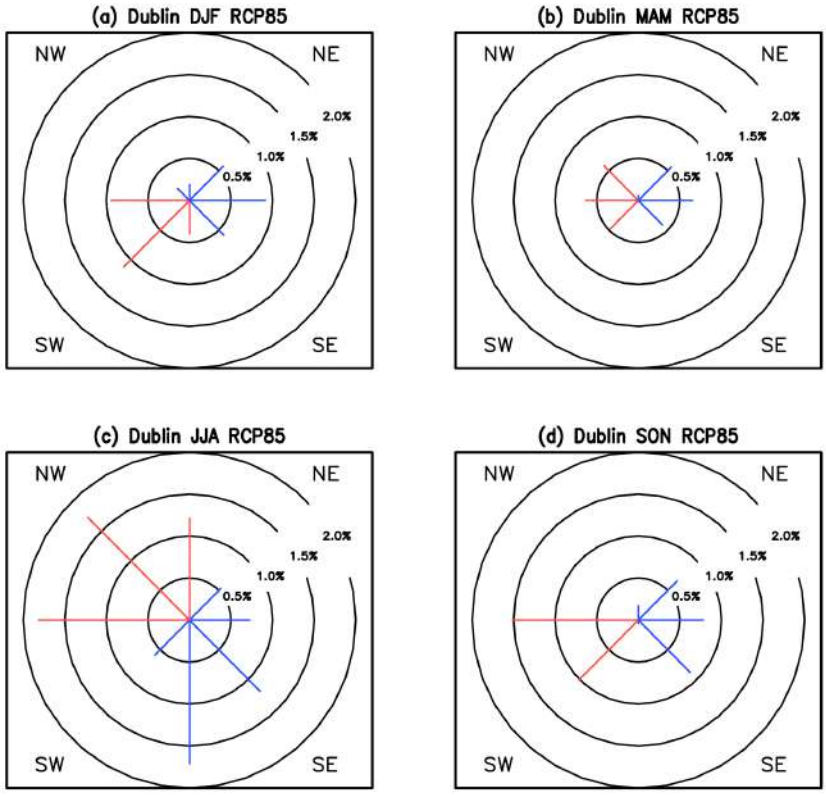

Figure 19: Projected multi-model mean changes in the frequency distributions of simulated wind directions in winter (DJF), spring (MAM), summer (JJA) and autumn between the periods 1971-2000 and 2040-2069 in Dublin under the RCP8.5 scenario. The changes are given in percentage points, with red bars depicting an increase and blue bars a decrease in the frequency. The circles indicate the scale of changes for each cardinal and intercardinal direction with an interval of 0.5%.

3.2.5 Climate change projections for Guilford

The climate projections for Guilford resemble those for Dublin in several aspects, but the changes are generally larger (Figures 2-4). The percentage increase in summertime diurnal temperature range is about twice as large as in Dublin, and annual mean solar radiation flux is projected to increase approximately at the same rate as in Bologna, although not as rapidly as in Bottrop and Hasselt, as we will see in the following.

In more detail, the seasonal mean temperature increases in Guilford are projected to range from 0.27 (0.13-0.41) °C decade^{-1} in spring to 0.40 (0.16-0.64) °C decade^{-1} in summer under the RCP8.5 scenario (Figure 20). In summer, the increases in daily maxima clearly exceed those in daily minima. Based on the multi-model mean estimates, little changes in precipitation amounts are expected in April and May and around October, but decreases in summer and increases in winter.

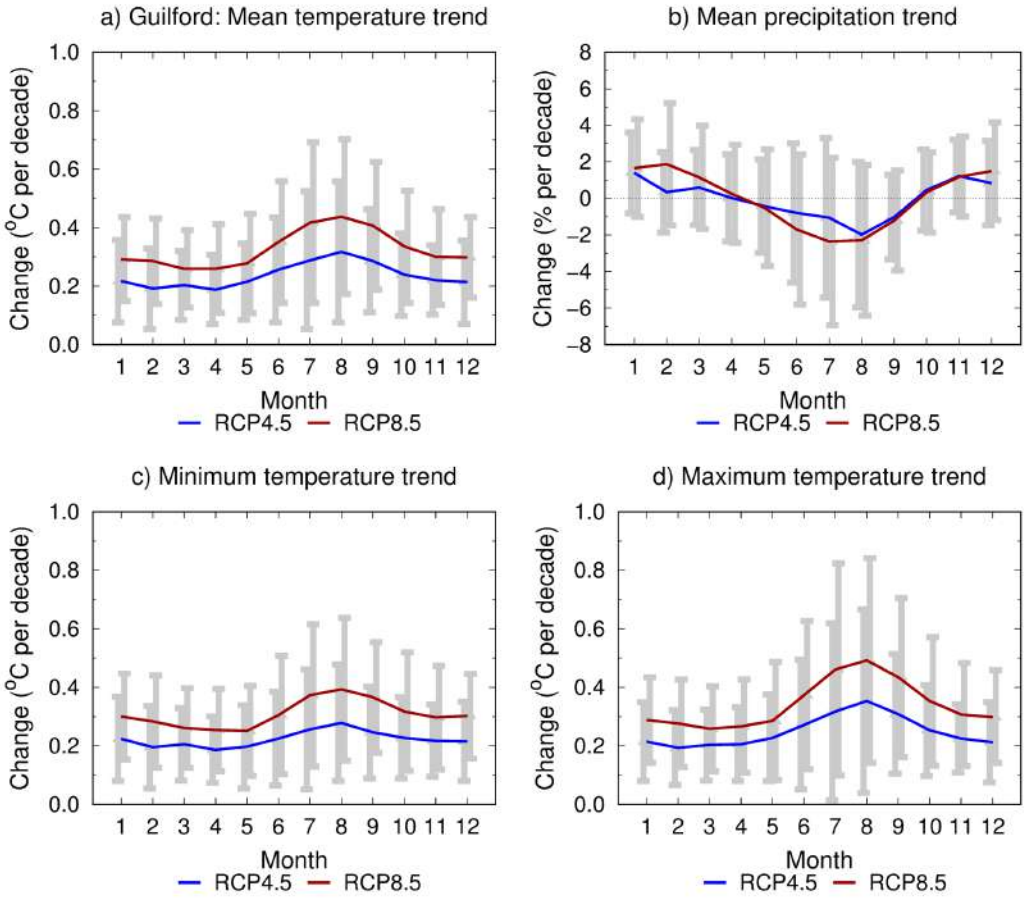

Figure 20: Projected trends in (a) monthly mean air temperature, (b) monthly precipitation total, (c) monthly mean of daily minimum temperature, and (d) monthly mean of daily maximum temperature between the periods 1981-2010 and 2040-2069 in Guilford under the RCP4.5 and RCP8.5 scenarios. The multi-model mean projections for each calendar month (1 = January, 12 = December) are depicted by solid curves (blue for RCP4.5 and red for RCP8.5). The grey bars indicate the 90 % uncertainty intervals for the change (left for RCP4.5 and right for RCP8.5).

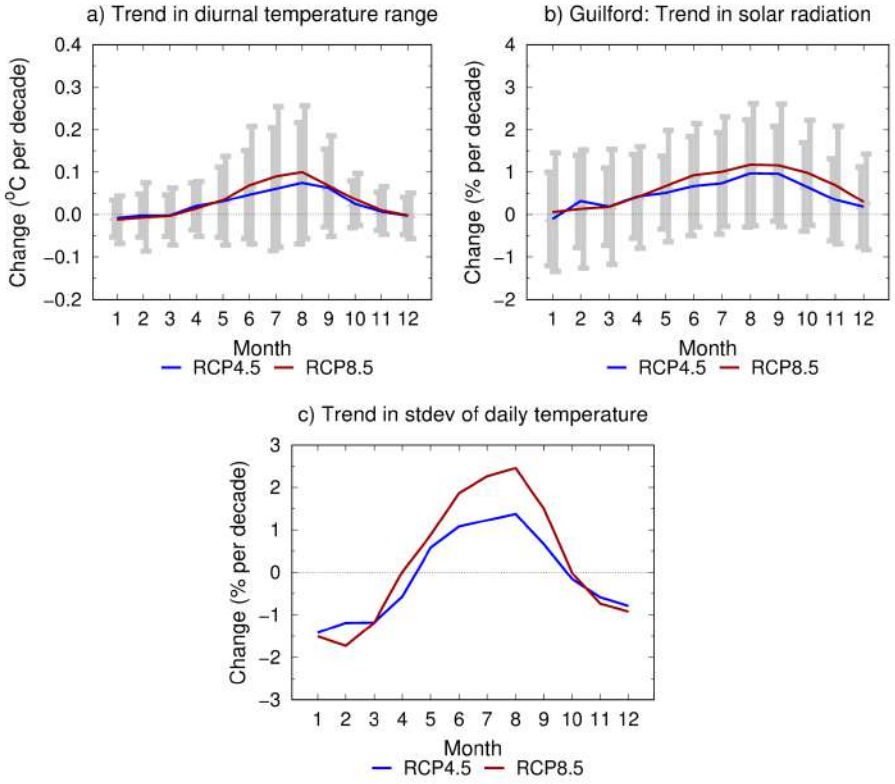

Figure 21: Projected trends in (a) monthly mean diurnal temperature range, (b) monthly mean incident solar radiation, and (c) monthly standard deviation of the temporal variability of daily mean temperature by the period 2040–2069 in Guilford under the RCP4.5 (blue) and RCP8.5 (red) scenarios. The baseline period is 1981-2010 (top) or 1971-2000 (bottom). For further information, see the caption for Figure 20.

In winter, since the projected increases in daily minimum and maximum temperatures are very similar, the diurnal temperature range remains virtually unaltered. Changes in solar radiation are likewise minor. In summer, both the diurnal temperature range, the temporal variability of daily mean temperature and incident solar radiation are projected to increase (Figure 21).

The multi-model mean estimates for changes in surface air pressure and mean wind speed are so small that there are few systematic differences between the two RCP scenarios considered in Figure 22. In winter, the portion of south-westerly winds is projected to increase slightly (Figure 23).

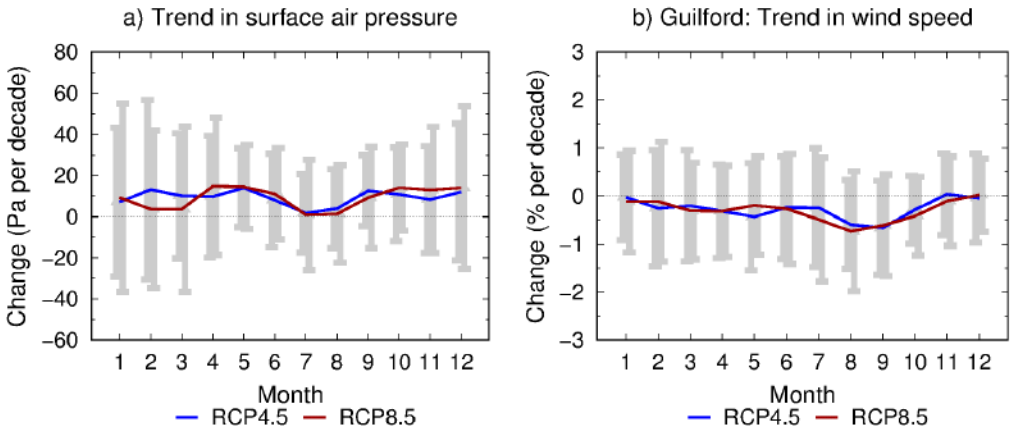

Figure 22: Projected trends in a) monthly mean surface air pressure and b) wind speed between the periods 1981-2010 and 2040-2069 in Guilford under the RCP4.5 (blue) and RCP8.5 (red) scenarios. For further information, see caption for Figure 20.

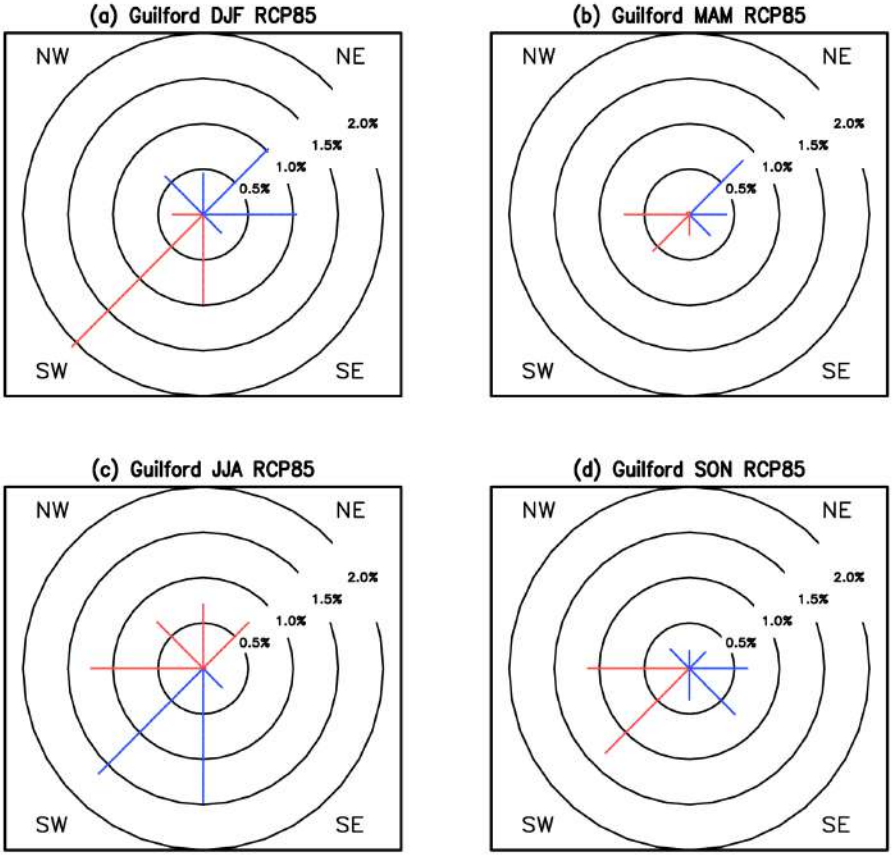

Figure 23: Projected multi-model mean changes in the frequency distributions of simulated wind directions in winter (DJF), spring (MAM), summer (JJA) and autumn between the periods 1971-2000 and 2040-2069 in Guilford under the RCP8.5 scenario. The changes are provided in percentage points, with red bars depicting an increase and blue bars a decrease in the frequency. The circles indicate the scale of changes for each cardinal and intercardinal direction with an interval of 0.5%.

3.2.6 Climate change projections for Hasselt

The climate projections for Hasselt are very similar to those for the nearest iSCAPE city, Bottrop. There is a general trend towards higher temperatures, particularly so in summer, slightly wetter winters and drier summers, more solar radiation and little changes in mean wind speed (Figures 2-6). The multi-model mean projections show some increases (decreases) in the portion of southwesterly winds in winter (summer) (Figure 7).

Based on the model simulations, the seasonal mean temperature trend under the RCP8.5 scenario is 0.35 (0.20-0.50) °C decade^{-1} in winter and 0.45 (0.20-0.70) °C decade^{-1} in summer (Figure 24). The multi-model mean estimates indicate decreases in precipitation from June to September but the inter-model differences are large. During those months increases in daytime temperatures typically clearly exceed increases in nocturnal temperatures, which result in increases in the diurnal temperature range (Figure 25). Also the day-to-day temperature fluctuations are projected to intensify at that time of the year, whereas in winter they are projected to attenuate. The projected increase in incident solar radiation in summer is 1.2 (0.0-2.4) % decade^{-1}.

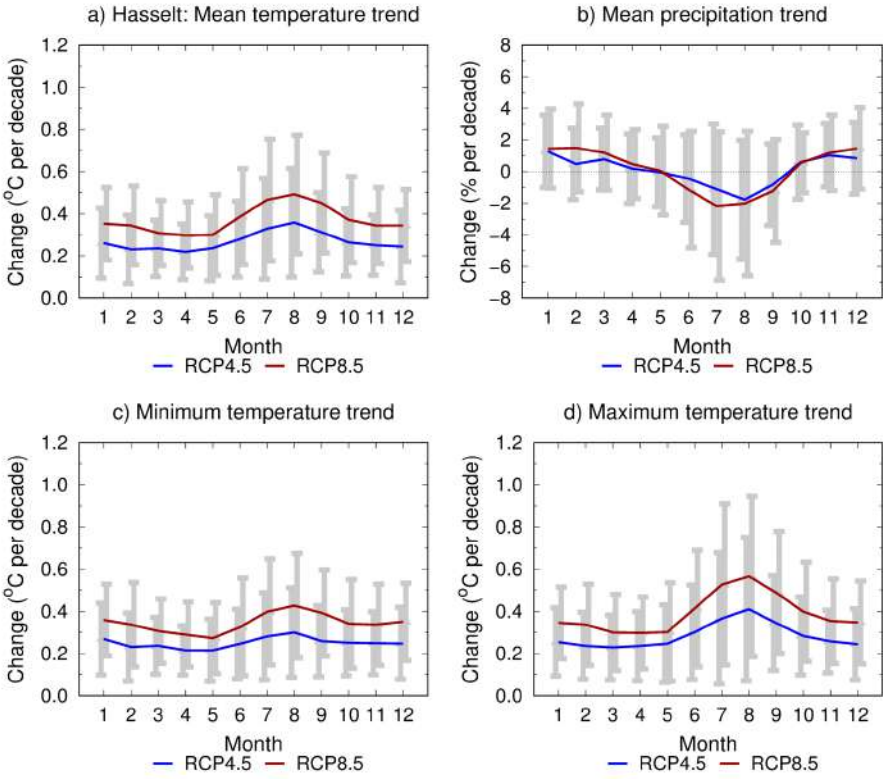

Figure 24: Projected trends in (a) monthly mean air temperature, (b) monthly precipitation total, (c) monthly mean of daily minimum temperature, and (d) monthly mean of daily maximum temperature between the periods 1981-2010 and 2040-2069 in Hasselt under the RCP4.5 and RCP8.5 scenarios. The multi-model mean projections for each calendar month (1 = January, 12 = December) are depicted by solid curves (blue for RCP4.5 and red for RCP8.5). The grey bars indicate the 90 % uncertainty intervals for the change (left for RCP4.5 and right for RCP8.5).

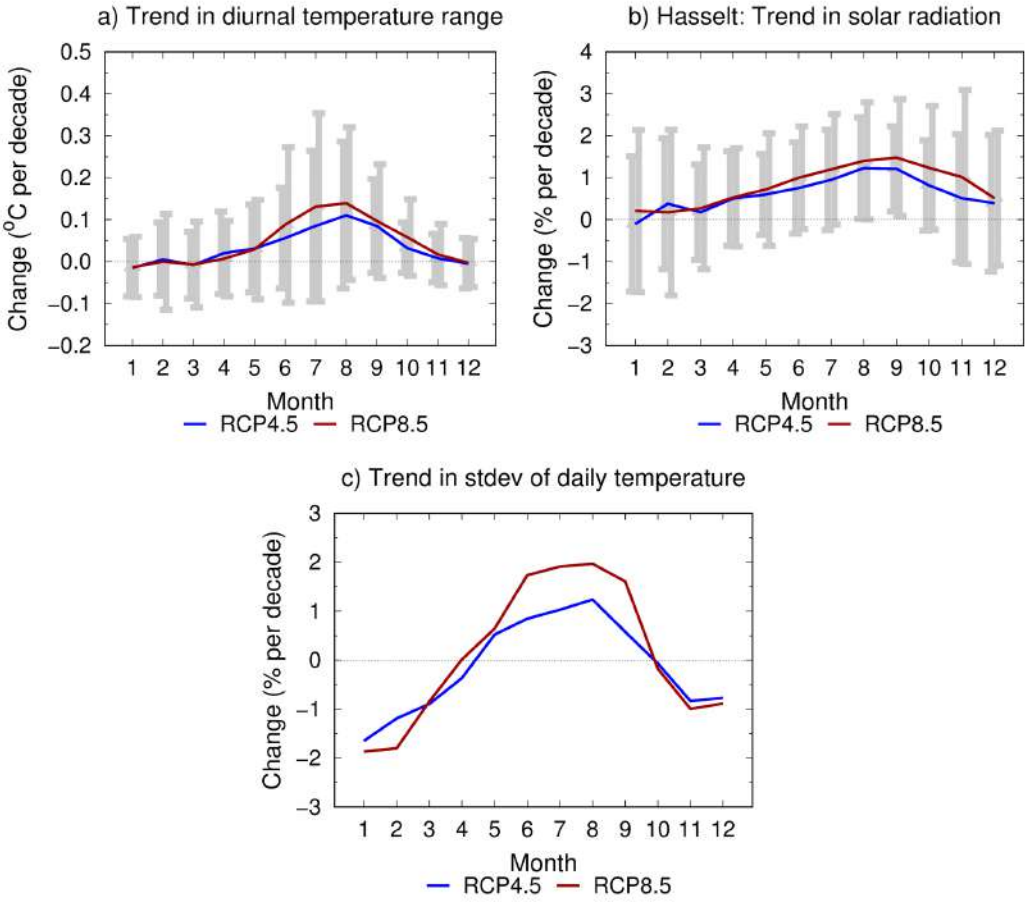

Figure 25: Projected trends in (a) monthly mean diurnal temperature range, (b) monthly mean incident solar radiation, and (c) monthly standard deviation of the temporal variability of daily mean temperature by the period 2040–2069 in Hasselt under the RCP4.5 (blue) and RCP8.5 (red) scenarios. The baseline period is 1981-2010 (top) or 1971-2000 (bottom). For further information, see the caption for Figure 24.

According to the multi-model mean estimates, the share of southwesterly winds would increase in winter and decrease in summer, by about 3 percentage points within seven decades (Figure 27). However, the monthly mean wind speeds would remain almost unchanged (Figure 26).

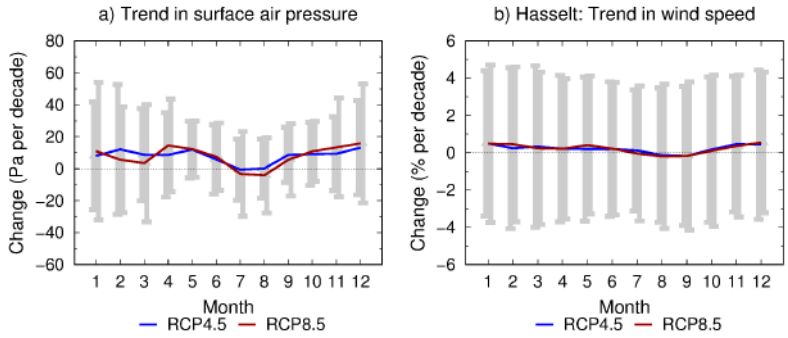

Figure 26: Projected trends in a) monthly mean surface air pressure and b) wind speed between the periods 1981-2010 and 2040-2069 in Hasselt under the RCP4.5 (blue) and RCP8.5 (red) scenarios. For further information, see caption for Figure 24.

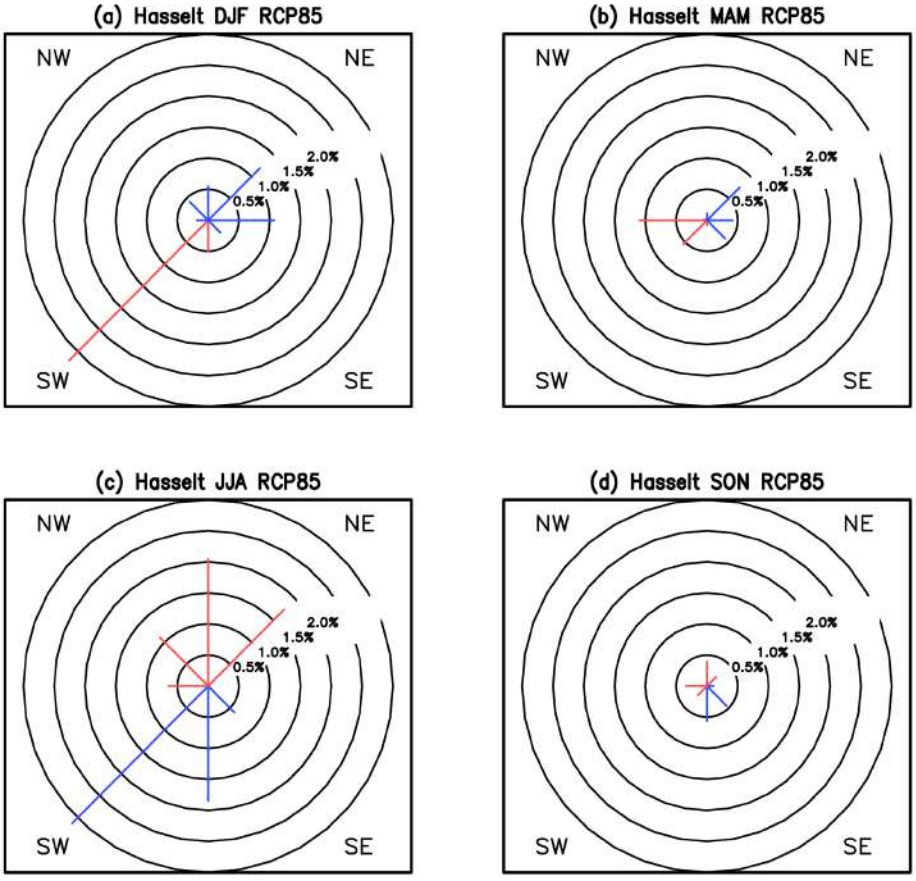

Figure 27: Projected multi-model mean changes in the frequency distributions of simulated wind directions in winter (DJF), spring (MAM), summer (JJA) and autumn between the periods 1971-2000 and 2040-2069 in Hasselt under the RCP8.5 scenario. The changes are provided in percentage points, with red bars depicting an increase and blue bars a decrease in the frequency. The circles indicate the scale of changes for each cardinal and intercardinal direction with an interval of 0.5%.

3.2.7 Climate change projections for Vantaa

The projected future changes in the climate of Vantaa deviate from those for the other iSCAPE cities. While the season with the largest projected warming, increases in diurnal temperature range and incident solar radiation, and decreases in precipitation is generally summer in the other cities, for Vantaa the season with the most pronounced changes is winter. In other words, the warming trend (Figure 3) and also the projected changes in precipitation and solar radiation are stronger in winter than in summer (Figure 4). Similar to the other cities, the multi-model mean changes in the mean wind speed are small compared to the uncertainty ranges.

In more detail, the projected seasonal mean warming ranges from 0.69 (0.40–0.97) °C decade^{-1} in winter to 0.46 (0.21–0.70) °C decade^{-1} in summer under the RCP8.5 scenario. Expectedly, the increases in daily mean, maximum and minimum temperatures are invariably lower under RCP4.5 than under RCP8.5 (Figures 28a, c, d). This is generally also true for changes in precipitation, except for summer (Figure 28b). In summer the signal of change is weak compared to inter-model differences and noise due to internal variability: the multi-model seasonal mean (the uncertainty interval) is 0.1 (-3.0…3.3) % decade^{-1}. In winter the seasonal mean rate of change is 2.5 (0.4-4.6) % decade^{-1}.

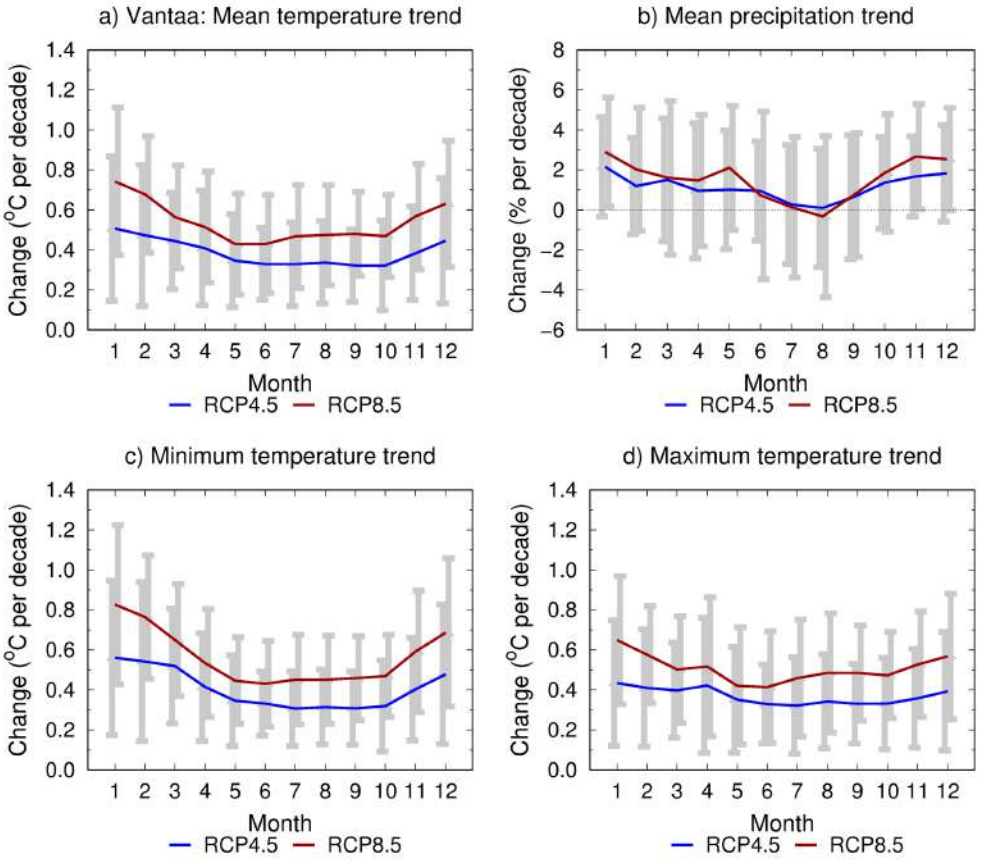

Figure 28: Projected trends in (a) monthly mean air temperature, (b) monthly precipitation total, (c) monthly mean of daily minimum temperature, and (d) monthly mean of daily maximum temperature between the periods 1981-2010 and 2040-2069 in Vantaa under the RCP4.5 and RCP8.5 scenarios. The multi-model mean projections for each calendar month (1 = January, 12 = December) are depicted by solid curves (blue for RCP4.5 and red for RCP8.5). The grey bars indicate the 90 % uncertainty intervals for the change (left for RCP4.5 and right for RCP8.5).

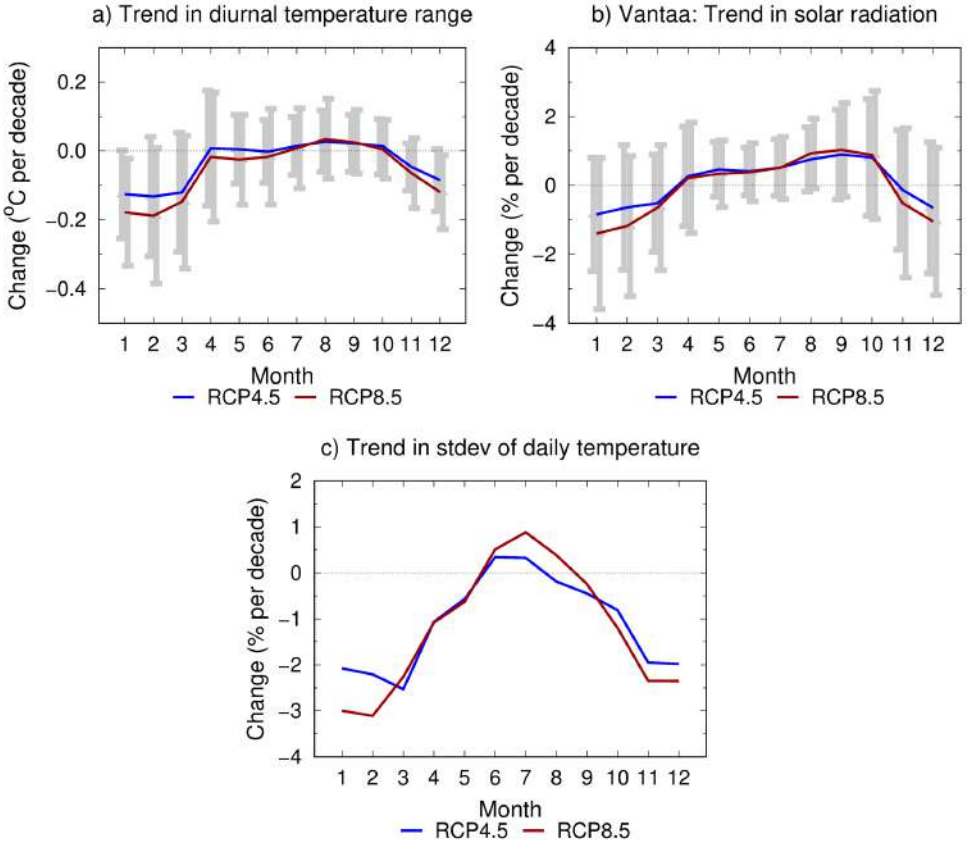

Figure 29: Projected trends in (a) monthly mean diurnal temperature range, (b) monthly mean incident solar radiation, and (c) monthly standard deviation of the temporal variability of daily mean temperature by the period 2040–2069 in Vantaa under the RCP4.5 (blue) and RCP8.5 (red) scenarios. The baseline period is 1981-2010 (top) or 1971-2000 (bottom). For further information, see the caption for Figure 28.

In winter, the diurnal temperature range is projected to decrease (Figure 29a), the rate of change being -0.16 (-0.30…-0.02) °C decade^{-1}. In the other seasons, the projected increases in daily maximum and minimum temperatures are close to each other and the diurnal temperature range alters little.

The projected changes in incident solar radiation (Figure 29b) resemble those for the diurnal temperature range. Both quantities are tightly linked with clouds. Increasing cloudiness reduces incident solar radiation as well as nocturnal infrared cooling, thereby cutting down the differences between the day- and night-time temperatures. The opposite is true for decreasing cloudiness. One can thus deduce that future winters in Vantaa would become even cloudier (and wetter; see Figure 28b) but early autumns slightly sunnier than in the recent past.

The day-to-day temperature fluctuations are projected to attenuate in the future not only in winter but also in spring and autumn (Figure 29c). Only in June and July do the multi-model estimates show small increases both under the RCP4.5 and RCP8.5 scenarios.

The multi-model mean projections mainly show slight decreases in monthly mean sea level air pressure (Figure 30a). The uncertainty in changes in monthly mean wind speeds is so large that multi-model mean projections deviate in sign between RCP4.5 and RCP8.5 (Figure 30b). In all seasons, the share of westerly winds is projected to slightly increase (Figure 31). The largest change in the frequency distributions of the simulated wind directions is projected to occur in

autumn, when the share (in %) of southwesterly winds would increase, in absolute terms, by about 1.5 % within seven decades.

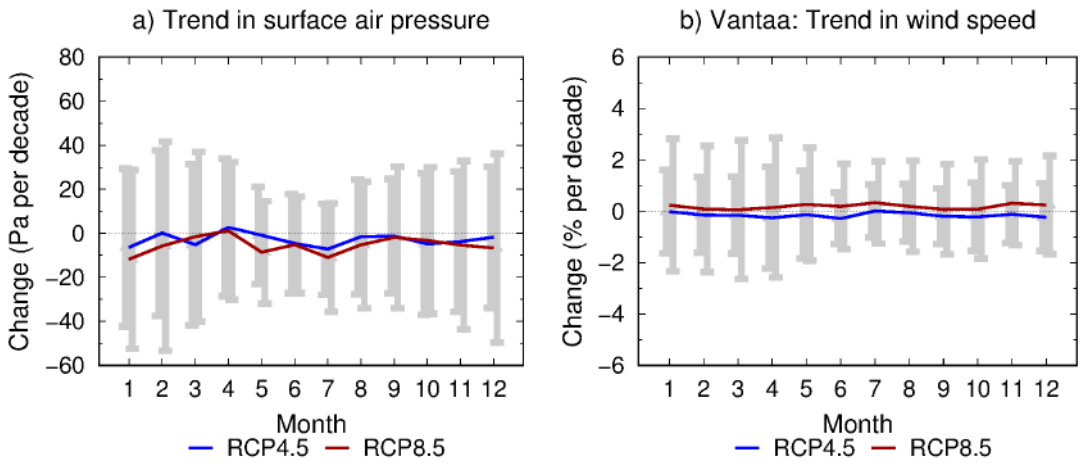

Figure 30: Projected trends in a) monthly mean surface air pressure and b) wind speed between the periods 1981-2010 and 2040-2069 in Vantaa under the RCP4.5 (blue) and RCP8.5 (red) scenarios. For further information, see caption for Figure 28.

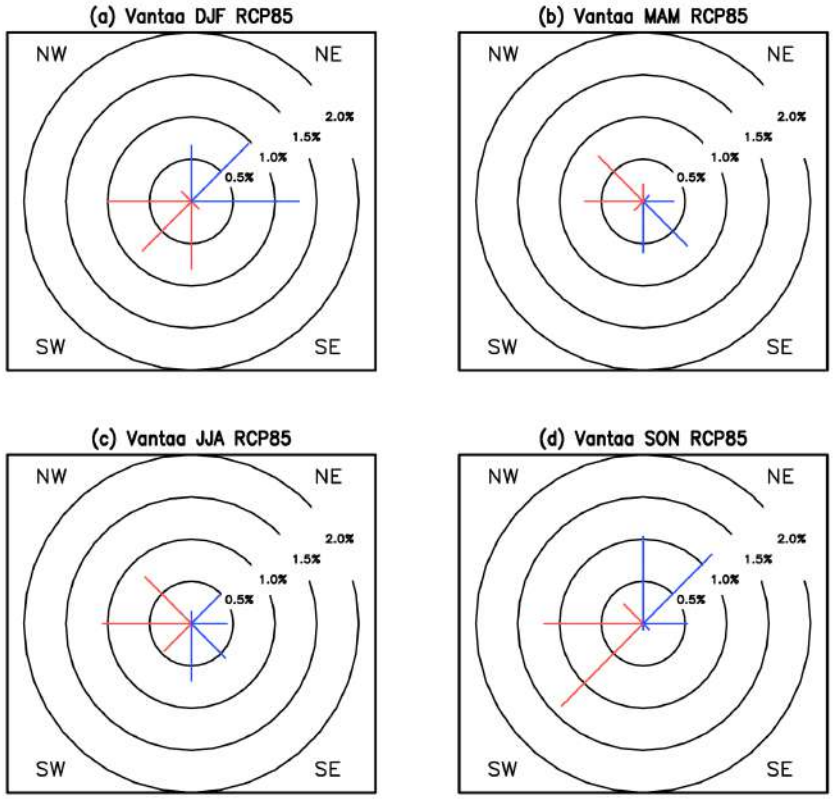

Figure 31: Projected multi-model mean changes in the frequency distributions of simulated wind directions in winter (DJF), spring (MAM), summer (JJA) and autumn between the periods 1971-2000 and 2040-2069 in Vantaa under the RCP8.5 scenario. The changes are provided in percentage points, with red bars depicting an increase and blue bars a decrease in the frequency. The circles indicate the scale of changes for each cardinal and intercardinal direction with an interval of 0.5%.

4 High-resolution simulations for Vantaa

The purpose of this section is to document a study about climatic impacts of a "Passive Control System" (PCS) intervention in one of the cities, Vantaa, in the current climate and in a projected future climate scenario. Similar high-resolution simulations could be made for any urban areas, provided that adequate resources were available for a number of mandatory preparatory phases.

Based on urban development models considered in iSCAPE D1.2 (Gharbia et al., 2018), Vantaa can be classified as a decentralised city, having a dispersed and mosaic settlement structure and no clear distinction between open spaces and built-up areas. Over 60% of the area of the city consists currently of green and blue spaces contrasting only 18% sealed surface. The classification for Vantaa differs from the other iSCAPE cities, as Bologna and Dublin are examples of a compact city, while Bottrop, Guilford and Hasselt are examples of a decentralised concentration. Therefore, the simulation results presented here for Vantaa cannot be directly generalized for the other European cities.

4.1 SURFEX module and the intervention considered

The consequences of altering urban characteristics in the city of Vantaa on local meteorological conditions in the present and projected future climate were studied by using the regional scale surface interaction module SURFEX (Masson et al., 2013). The Town Energy Balance (TEB) model (Masson, 2000; Lemonsu et al., 2004), included in SURFEX, is a model capable of clearly separating buildings, air within urban canyons, roads, and, if present, trees, gardens etc. This is crucial, since interactions of the atmosphere with the Earth's surface via fluxes of heat, momentum and various species depend on the underlying surface.

In iSCAPE, SURFEX was deployed over a roughly square domain, having a size of 38 x 42 km, situated on the southern coast of Finland, with the city of Vantaa in the middle (Figure 32). The applied grid spacing was 500 m by 500 m.

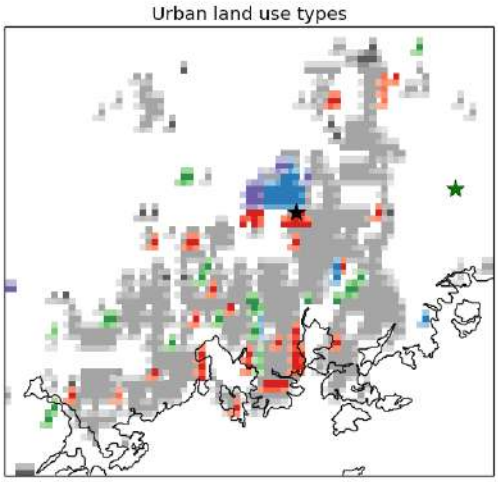

Figure 32: Urban land use types over the domain of SURFEX. Suburban types are shown in grey, commercial and industrial areas in red, parks and sports facilities in green, and airports and ports in blue color. The commercial area of Vantaa Tikkurila and the forest of the Sipoonkorpi National Park are shown by black and green stars, respectively.

The intervention of increasing the share of green spaces consisted in replacing all relatively dense commercial and industrial areas (shown in red color in Figure 32) with a suburban type, featuring lower and less dense buildings and a larger fraction of vegetated spaces (Table 2). The changes in urban characteristics are not extreme and take place only over limited areas. Therefore, the effects are to be expected mainly in the street canyons immediately affected. In particular we do not expect the changes to have a significant impact on the whole urban boundary layer. Therefore the same atmospheric forcing (Section 4.2) may be applied to SURFEX before and after the intervention.

	Building fraction	Building height (m)	Vegetated fraction	Wall surface ratio
Baseline	0.45	20	0.1	0.45
Intervention	0.28	10	0.44	0.28

Table 2: Urban characteristics at Vantaa Tikkurila before and after the intervention of lower and less dense buildings and more widespread green space.

4.2 Methodological approach for the current climate

The baseline period considered in the simulations consists of an artificially constructed test reference year representing the recent past climate (Kalamees et al., 2012). The year has been constructed out of 12 historical months that were chosen from the period 1980-2009 in such a way that the monthly cumulative frequency distributions of daily mean air temperature, relative humidity, solar radiation and wind speed were as close as possible to their respective climatological, i.e. 30-year average, cumulative frequency distributions. The months selected are listed in Table 3.

Jan	Feb	Mar	Apr	May	Jun	Jul	Aug	Sep	Oct	Nov	Dec
1990	1998	1994	2009	2006	2005	2008	2003	1997	1981	1989	1998

Table 3: The months of the climatological test reference year for Vantaa (Jylhä et al., 2011)).

Hourly time series of meteorological data (forcing data), needed to run SURFEX, were generated for the test year by the HARMONIE-AROME configuration of the ALADIN-HIRLAM numerical weather prediction system (Bengtsson et al., 2017). Short-range hind-casts were produced four times for each day of the respective months of the test-year, and hourly series of air temperature, humidity, wind speed, rain, snowfall, as well as down welling solar and thermal radiation were extracted for the SURFEX domain.

4.3 Verification

The simulated test-year weather data was verified using observations from the Helsinki-Vantaa airport meteorological station (WMO station number 02974). The mean differences between simulations and observations and the correlation coefficients for the whole test-year can be seen in Table 4. The table indicates that the models are able to simulate temperature very well, while humidity and wind speed are simulated quite well. The models are capable of predicting precipitation fairly well.

Simulated variable (unit)	Temperature (°C)	Humidity (%)	Wind speed (m/s)	Precipitation (mm/12 h)
Mean difference from the observation	0.07 ± 0.03	0.15 ± 0.14	-0.53 ± 0.02	-0.24 ± 0.07
Correlation coefficient	0.984	0.876	0.835	0.783
p-value	< 0.001	< 0.001	< 0.001	< 0.001

Table 4: The mean differences and correlation coefficients, with p-values, between the modelled test-year data and the observed meteorological variables at the Helsinki-Vantaa airport meteorological station. The mean differences are calculated using the data of the whole test-year.

In Figure 33 the diurnal temperature variations are shown separately for all four seasons. The seasons all contain three months, winter containing December, January and February. As the measurements originate from different years and even different decades (Table 3), there are some differences in the measurement intervals. Therefore, the figure depicting summertime daily variation (upper right panel) has data for every hour and the other seasons for 3-hour intervals.

The autumn daily temperature variation (Figure 33, lower left panel) seems to be modelled quite well, as the modelled temperature lines up well with the measurement, showing an average diurnal range of about 3.5 °C for the test year. For spring (upper left panel), the situation is almost equally good, but the temperature tends to be somewhat too low at night. The average diurnal temperature range is about 7 °C (8 °C) according to the measurements (simulations).

For summer (upper right panel), the modelled daily temperature variation has almost the same shape as the measured one, but the midday temperatures are about 1–1.5 °C too high. Accordingly, the observed average diurnal temperature range of about 7 °C is overestimated by the same amount.

In winter (lower right panel) the midday temperature peak is well modelled, while during the rest of the day the simulated temperature is almost one degree too cold. Compared to the other seasons, the average diurnal temperature range is quite narrow in winter according to both the observations and the simulation.

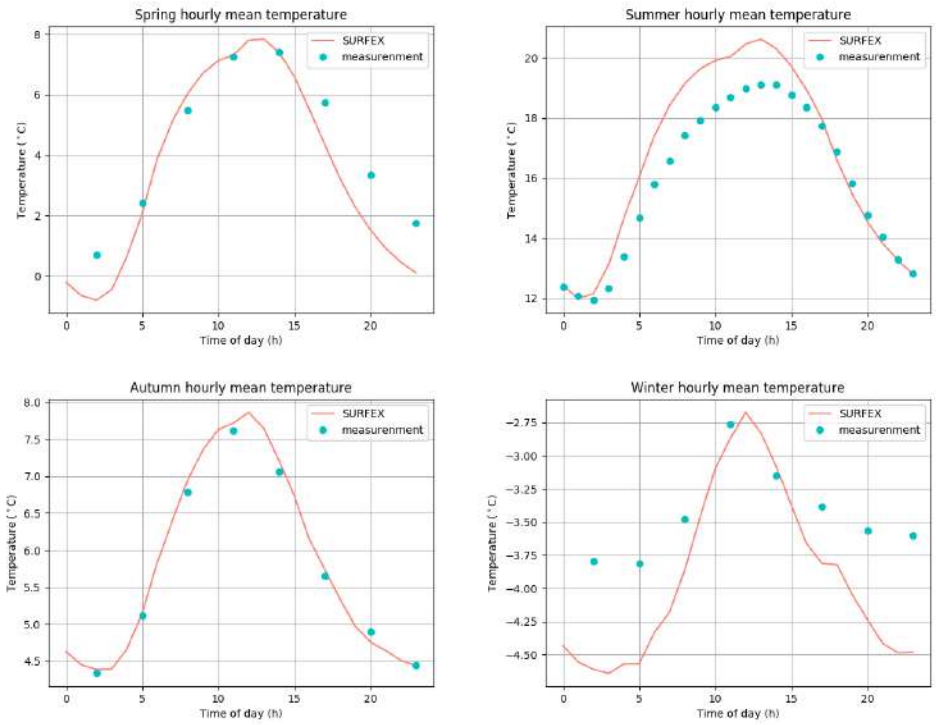

Figure 33. Observed and modelled seasonal mean diurnal temperature cycles at the Helsinki Vantaa airport for the test year. Note the different vertical scales in the diagrams.

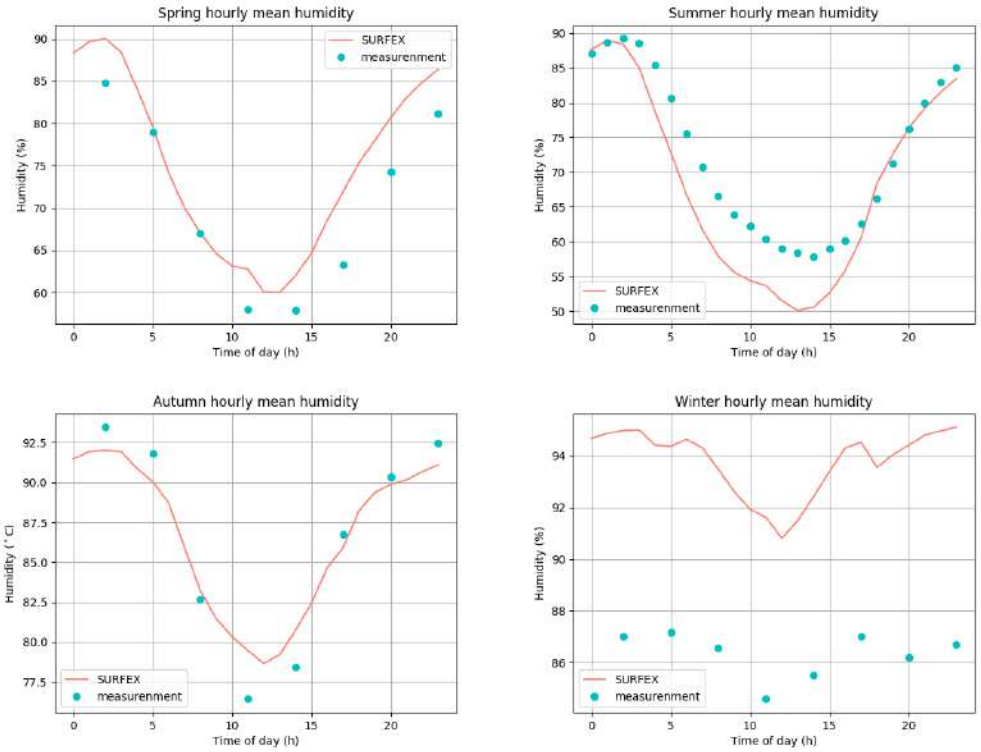

Figure 34: *Observed and modelled seasonal mean diurnal cycles of relative humidity at the Helsinki Vantaa airport for the test-year.*

For relative humidity (Figure 34), the best correspondence between observations and the model output is again found during spring and autumn (upper and lower right panels). During summer (upper right panel), the relative humidity starts to decrease too early in the morning and reaches too low values during midday. In winter (lower right panel), the model remains excessively moist throughout the day.

The simulated wind speed (Figure 35) displays a realistic diurnal cycle in all seasons, although the midday maxima tend to be slightly underestimated. A potential factor contributing to the underestimation is that the airport weather station area may have a smaller roughness length than assumed in the simulation.

The observed and simulated precipitation are compared in Figures 36 and 37. 12-hourly totals (Figure 36) are usually well predicted regarding the magnitude and timing during autumn, winter and spring, when most of the precipitation is related to the passage of frontal weather systems. In summer, when smaller-scale convective systems predominate, larger discrepancies occur, and the HARMONIE-AROME tends to underestimate precipitation. The same pattern is seen in the monthly totals shown in Figure 37.

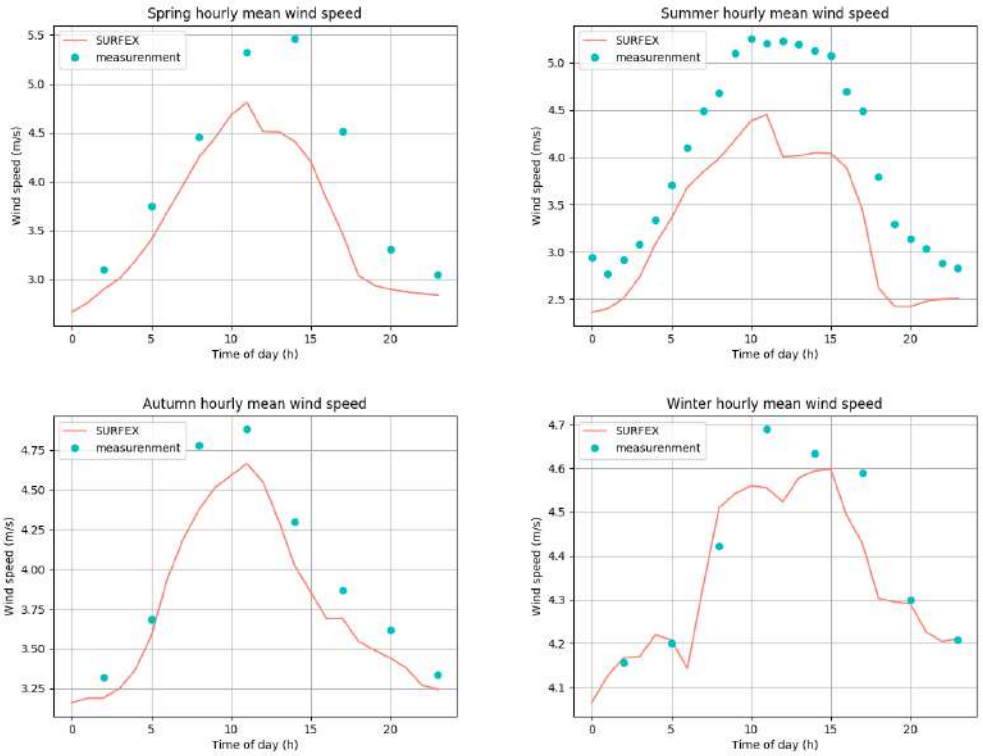

Figure 35: *Observed and modelled seasonal mean diurnal cycles of wind speed at Helsinki Vantaa airport for the test-year.*

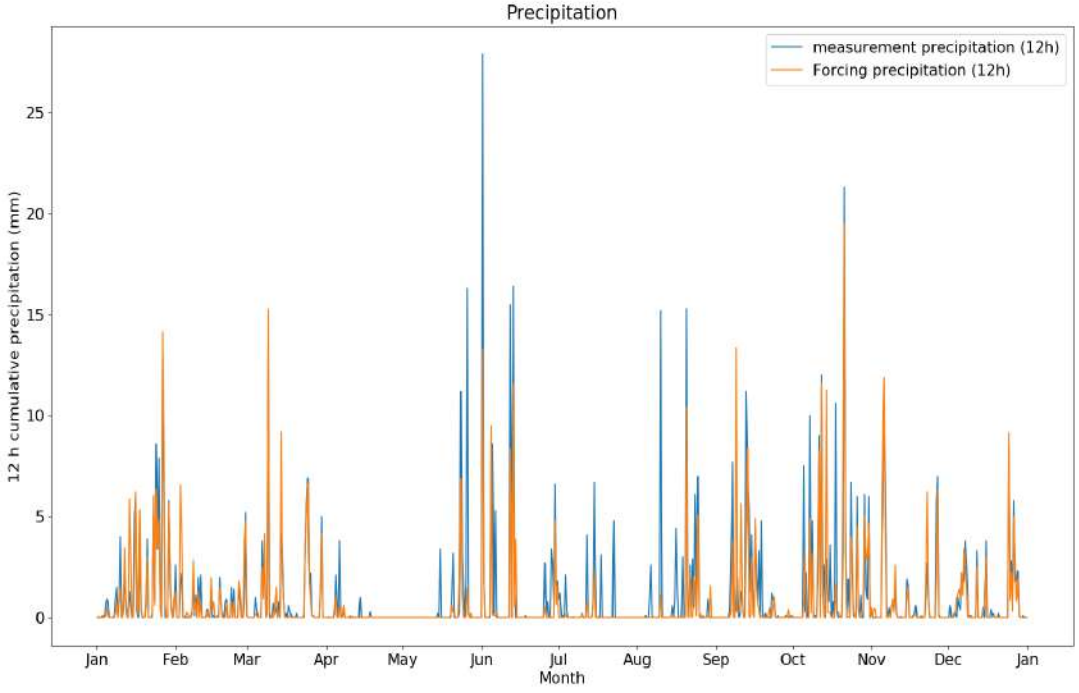

Figure 36: *Observed and modelled 12-hourly precipitation totals for the test-year.*

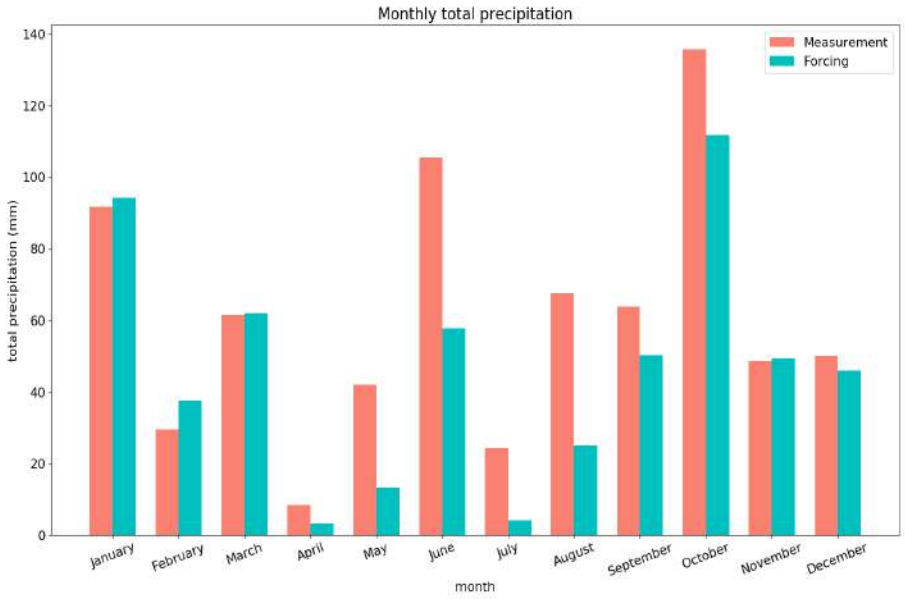

Figure 37: Observed and modelled monthly precipitation totals for the test-year.

4.4 Methodological approach for the future climate

Forcing data for the 2050s climate was generated by modifying the baseline test-year forcing with approaches that fall into the category of morphing or time series adjustment, discussed in Belcher et al. (2005). We customized two of five delta change methods previously examined by Räisänen and Räty (2013). The main objectives of the customized procedures were 1) to minimize the influence of climate model biases; 2) to realistically describe temporal fluctuations of weather from day to day and hour to hour, including inter-dependencies among the different climate variables; and 3) to ensure that the statistical properties of the scenario forcing data are consistent with the climate model projections for changes in mean values and (for temperature) variability. The methods for developing synthetic hourly temperature, wind speed and direction, total precipitation and shortwave radiation data are described in detail by Jylhä et al. (2015a), Jylhä et al. (2015b) and Lehtonen et al. (2014). The monthly mean changes in those climatic variables, needed in the time series adjustment, are shown in Section 3.2.7 of this report. The temporal evolution of the global GHG emissions and concentrations was assumed to follow the Representative Concentration Pathway RCP8.5 (Figure 1).

The hourly proportions of precipitation in the form of snow and rain were approximated by a linear function of the projected future temperature: P_S=kT+b, $T \in$ [-0.5 °C, 2.0 °C,], where P_S is the proportion of snow from total precipitation, T is the projected future temperature, and k and b are fit parameters calculated from the baseline temperature, rainfall and snowfall data in the HARMONIE-AROME simulations. Below -0.5 °C P_S is 1.0 and above 2.0 °C it is 0. For longwave radiation, an iterative method was developed to calculate the changes. In this calculation, the relation between original longwave and humidity forcings was used together with the changes for humidity data. A detailed presentation of the method can be found in the master's thesis by Saranko (2019).

Monthly averages of the meteorological forcing for the months of the test-year and as modified to account for the altered climate of the mid-2050s following RCP8.5 are shown in Figure 38 for the location of Helsinki-Vantaa airport. Clearly, the temperature is the parameter most seriously affected, displaying a warming of a few degrees throughout the annual cycle. For the test-year, all the winter months from December to March show mean temperatures well below freezing, while for the altered climate, this is true only for February. The more modest, but equally systematic, change in relative humidity indicates that the moisture content must be increasing throughout the year. Consistently with the increasing moisture content, downwelling terrestrial radiation is likewise predicted to increase throughout the year. Little change is seen in the wind speed. From October to January, the amount of precipitation increases by about 10%, while the summer months are less affected. It is worth keeping in mind, however, that summer precipitation in the baseline test-year forcing data remains well below the measured amounts (Figure 37).

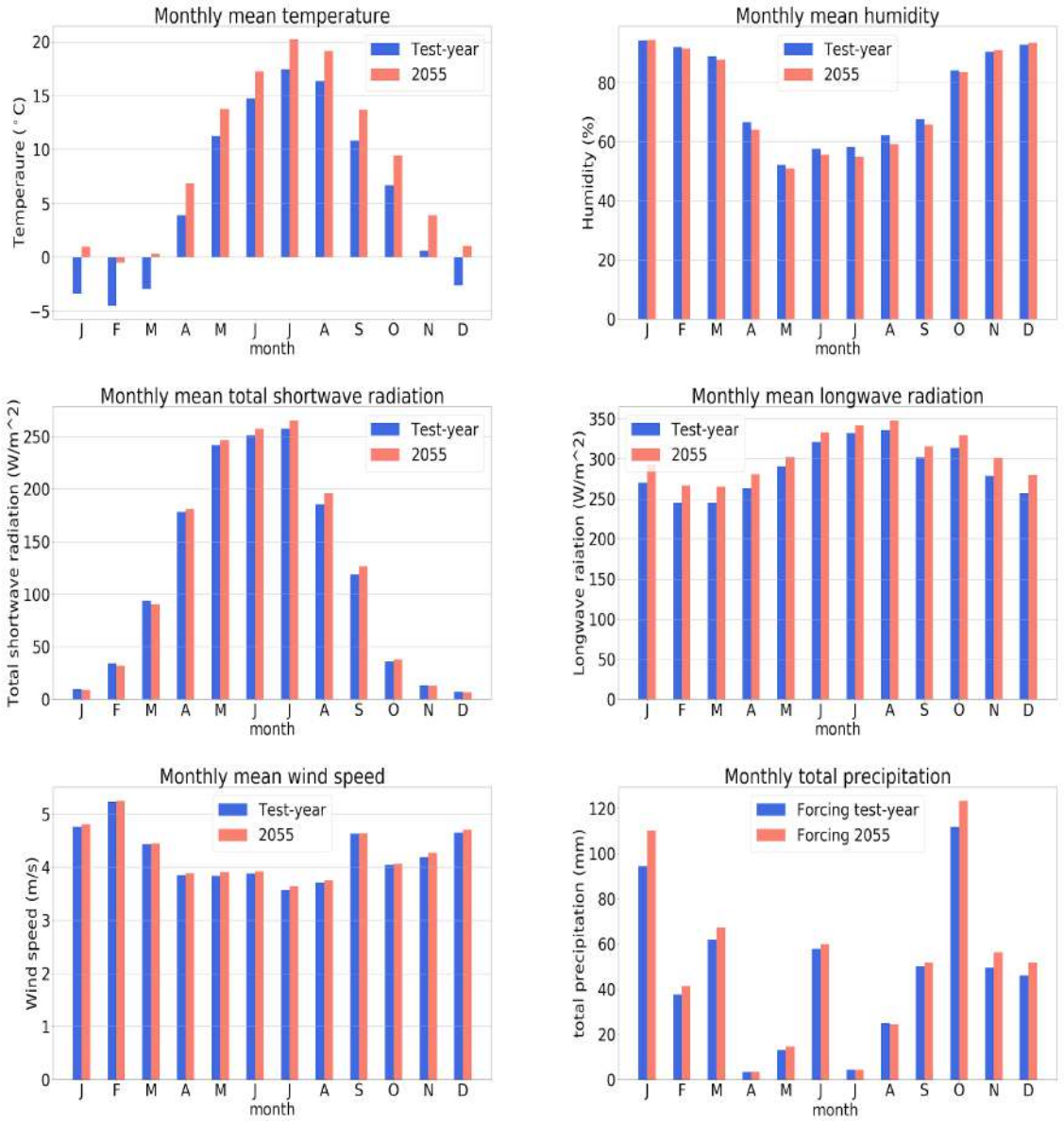

Figure 38: Monthly averaged meteorological forcing extracted from the simulated data for the Helsinki-Vantaa airport. Blue: as given by HARMONIE during the test-year. Red: as incremented to represent the mid-2050s climate according to RCP8.5. Panels from top left to bottom right show, respectively air temperature, relative humidity, insolation, downwelling terrestrial radiation, wind speed, and precipitation amount. Temperature, humidity, and wind speed represent conditions at 12 m above ground.

4.5 Modelled impacts of climate change and green infrastructure

4.5.1 Impacts of climate change, current green spaces

Concurrently, in the present climate, the presence of built-up areas in the Helsinki-Vantaa region has a pronounced effect on the simulated climate near the ground. Air temperature is generally higher, relative humidity lower and winds weaker in the built-up areas than in the surrounding agricultural and forested areas. For air temperature and humidity, the urban influence is strongest during the summer month (July, left panel in Figure 39); in January (left panel in Figure 40), the influence is weaker and the distance to the Gulf of Finland tends to dominate the spatial distribution. The urban weakening of the wind speed, by contrast, is most pronounced during winter, when winds are strongest on an average.

The same patterns as found for the current climate (left panels in Figures 39-40) are apparent in the projected future climate, in other words, when SURFEX is subjected to the altered forcing representing the mid-2050s. However, the presence of built-up areas tends to reduce the associated (absolute) changes in temperature and humidity in July, and in wind speed in January and July (right panels of Figures 39-40). For the averages over 500 m x 500 m grid squares considered, the effects are quite small, amounting to one or two tenths of a degree and one or two percent for temperature and relative humidity, respectively, and to about one cm per second for wind speed.

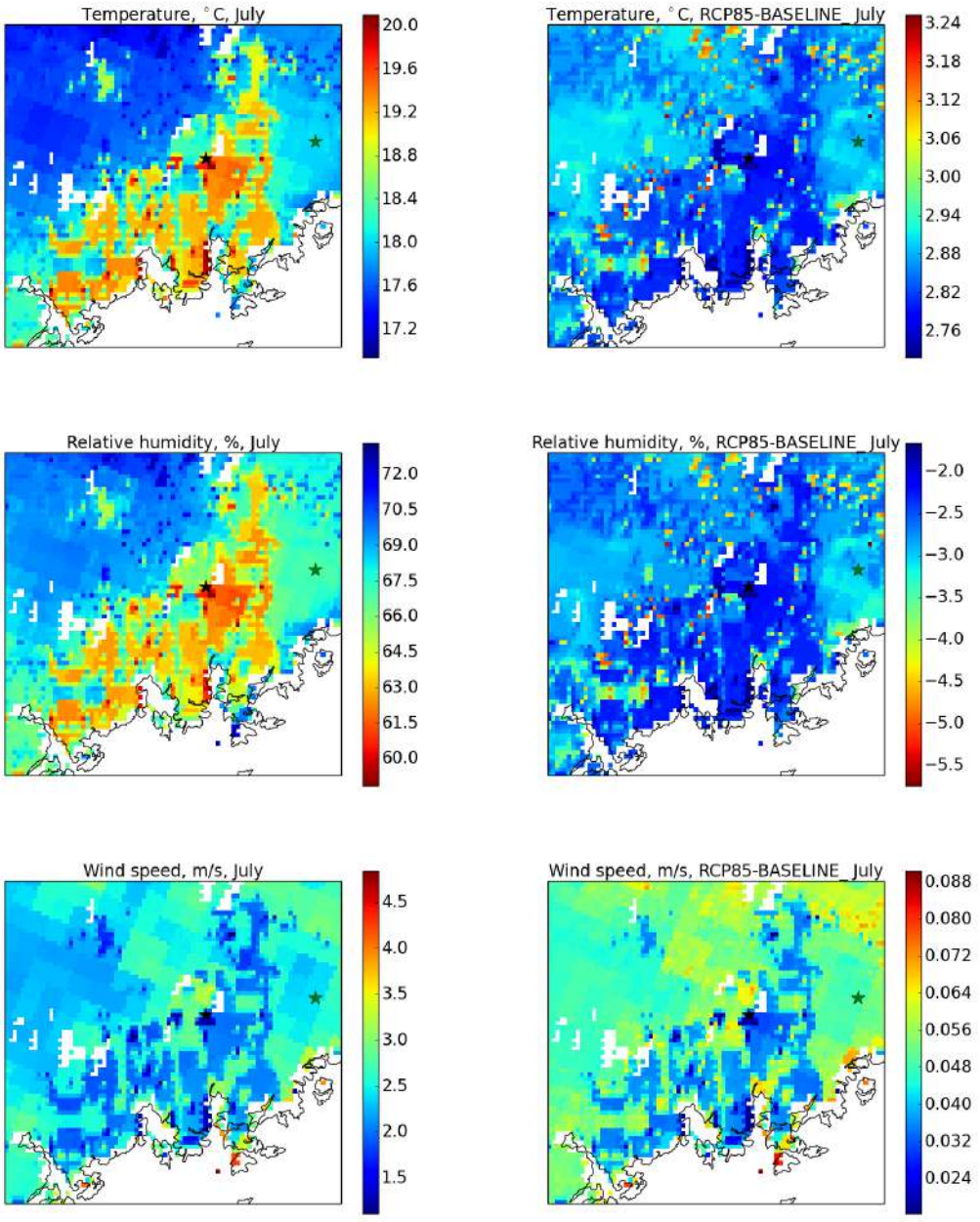

Figure 39: Monthly mean air temperature (top), relative humidity (middle) and wind speed (bottom) as simulated by SURFEX in July. Conditions of the test-year, representing current climate, are shown on the left. The high-resolution changes induced by the altered forcing, i.e., regional-scale climate change, are shown on the right. The commercial area of Vantaa Tikkurila and the forest of the Sipoonkorpi National Park are shown by black and green stars, respectively.

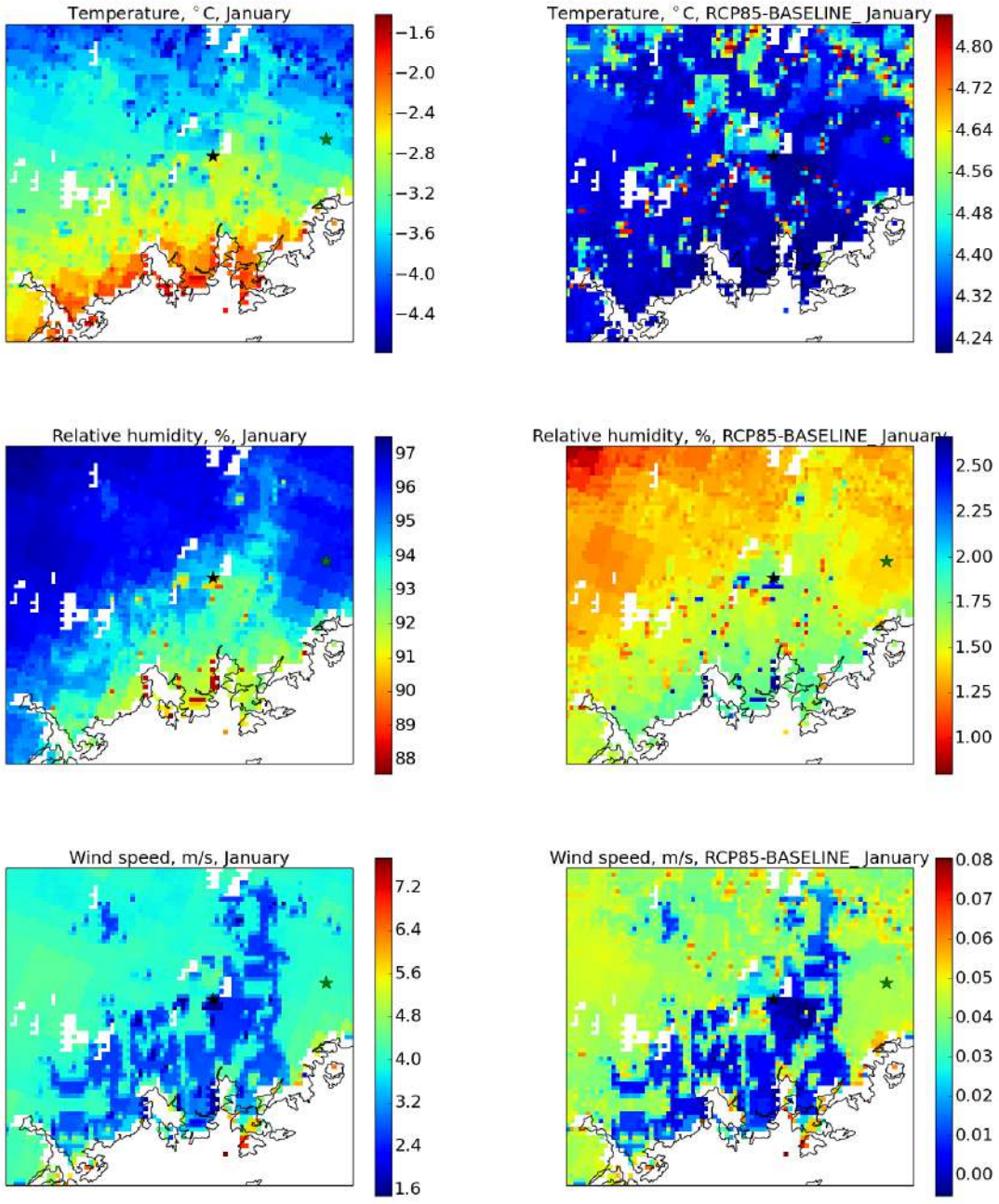

Figure 40: As Figure 39, but for the month of January.

4.5.2 Impacts of the intervention in the present climate

The impact of the intervention to alter key urban characteristics (Table 2) is explored in a 500 m by 500 m grid cell representing the Tikkurila area in central Vantaa, indicated by a black star in Figures 32, 39 and 40. Consequences of the intervention in the present climate are examined for July (Fig. 41, left column) and January (Fig 41, right column). For temperature and humidity, the effect of replacing the dense urban layout by a suburban type structure is quite modest but very systematic. On average, the air temperature drops by less than half a degree in January and by more than half a degree in July. In both summer and winter, the change is nearly independent of temperature. On average, relative humidity increases by about 3 percentage points in summer and winter, but the effect in winter is more variable. The main effect can be seen in the wind speed, which is almost doubled when the sheltering effect of the buildings is reduced.

The modest effect on temperature and humidity is an expected result, as the imposed changes to the urban morphology are rather modest and confined to very small areas. Vantaa is by no means a big city, and the difference between “urban” and “suburban” areas is not too dramatic. Moreover, the meteorological forcing was applied over an area of about 6.25 square kilometres and is not influenced by the intervention at all in our study. The strongest effects would probably be very local and related to individual structures such as buildings, or stands of trees, and remain unresolved in our experiment.

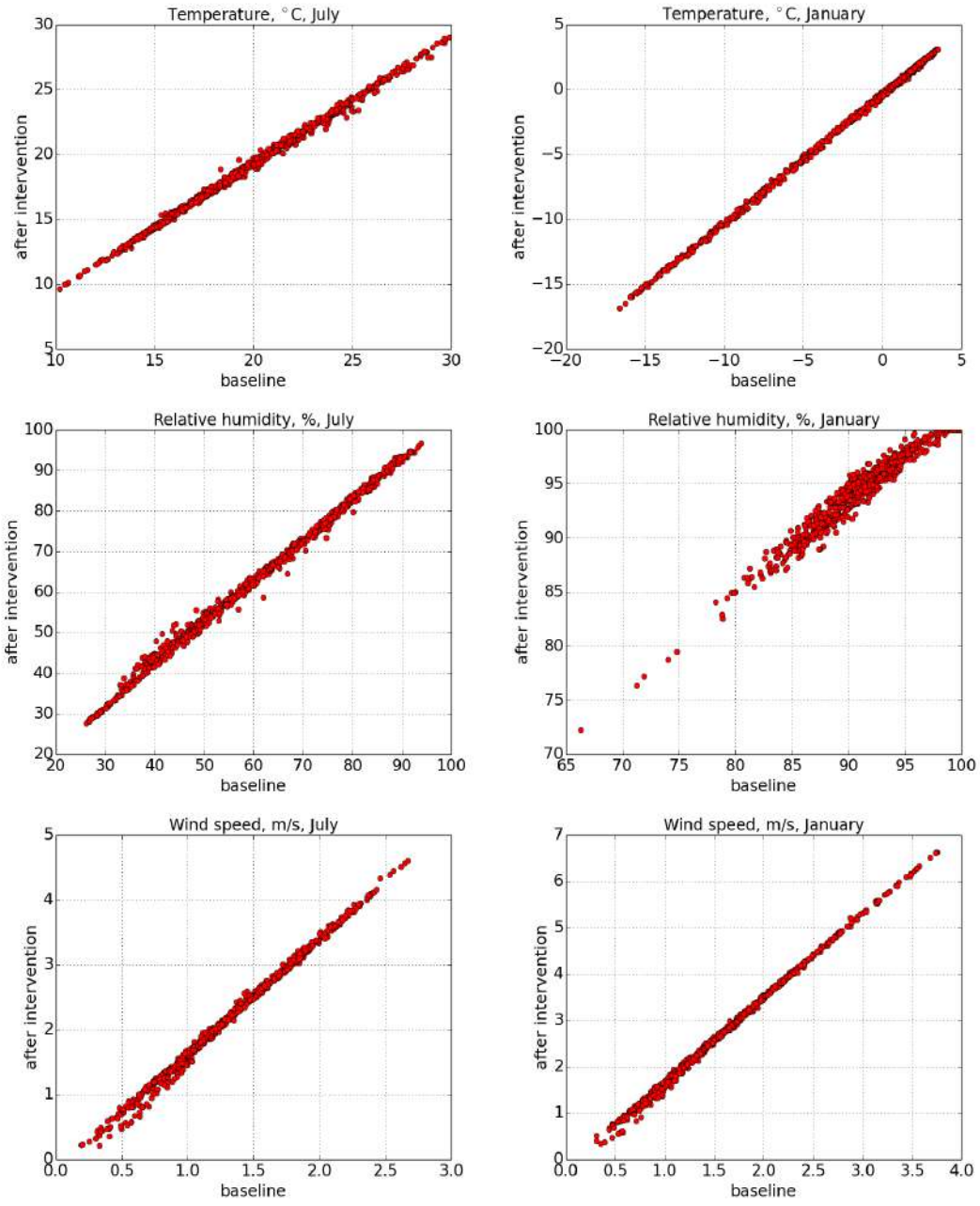

Figure 41: Scatter plots of air temperature (top panels), relative humidity (middle panels) and wind speed (bottom panels), showing the response to changing the urban layout in SURFEX for Tikkurila in Vantaa in July (left hand column) and January (right hand column).

4.5.3 Impacts of the intervention under changing climate

Simulated meteorological conditions at Vantaa Tikkurila, in the present climate and in the mid-2050s, with and without the intervention, are shown in the form of mean diurnal cycles in Figure 42. For temperature, the impact causes a warming of at most about one degree in the afternoon in July, whereas the impact of changing forcing (climate warming) amounts to several degrees in both months. In July, the intervention causes an increase of relative humidity throughout the day, amounting to about 3-5% in the afternoon, while climate change is associated with a drying of a similar magnitude. Conversely, in January, the intervention and climate change are both associated with a moistening of a few percentage units. Looking at wind speed, the intervention leads to an increase of about 0.5-2.5 m/s, while the impact of climate change is very small. Thus, changes in the atmospheric forcing (due to larger-scale changes in climate) tend to dominate for temperature, while changes in urban morphology dominate for wind speed. For the relative humidity, changing forcing and changing morphology are of comparable magnitude but of opposite sign in summer.

In Figure 43, simulated meteorological conditions at Vantaa Tikkurila, in the present climate and in the mid-2050s, with and without the intervention, are compared to conditions in the forested area of Sipoonkorpi National Park, at a comparable distance from the coast. Sipoonkorpi National Park is characterized by a mixed forest typical of southern Finland. Looking at the mean diurnal cycles, it can be observed that the intervention acts to reduce the difference between town and country by some 0.5-1 degrees in both January and July, while climate change causes a reduction of about 0.1 degrees (afternoon in July) or less. Relative humidity is lower in Tikkurila than in Sipoonkorpi in July and January, and the intervention acts to reduce the difference in both months by some 3-5 percentage units, while climate change acts to reduce the difference by about 2 units in the afternoon in July, at most. For wind speed, the difference between the two locations is reduced by the intervention by more than 1 m/s in January and slightly less in July. The effect of changed forcing amounts to less than 0.5 m/s. Thus for July and January, we can say that the urban morphology is the dominating factor controlling the difference between the town and the forest, changing climate being of secondary importance.

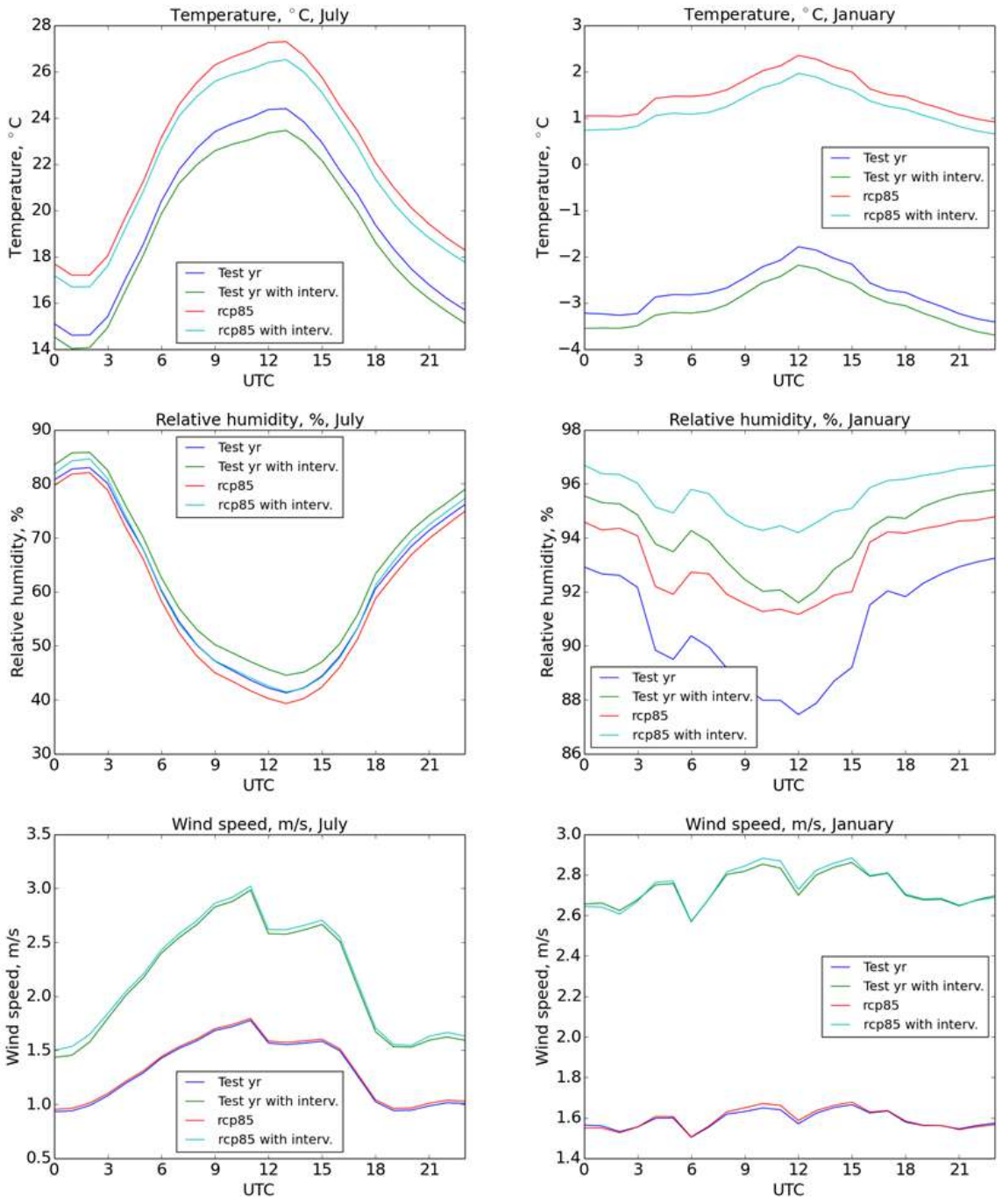

Figure 42: Monthly mean diurnal cycles of air temperature (top panels), relative humidity (middle panels) and wind speed (bottom panels), showing the response to changing climate and urban layout in SURFEX for Tikkurila in Vantaa in the months of July (left hand column) and January (right hand column). Local midday occurs at about 10 UTC. Note the different scales on the y-axes.

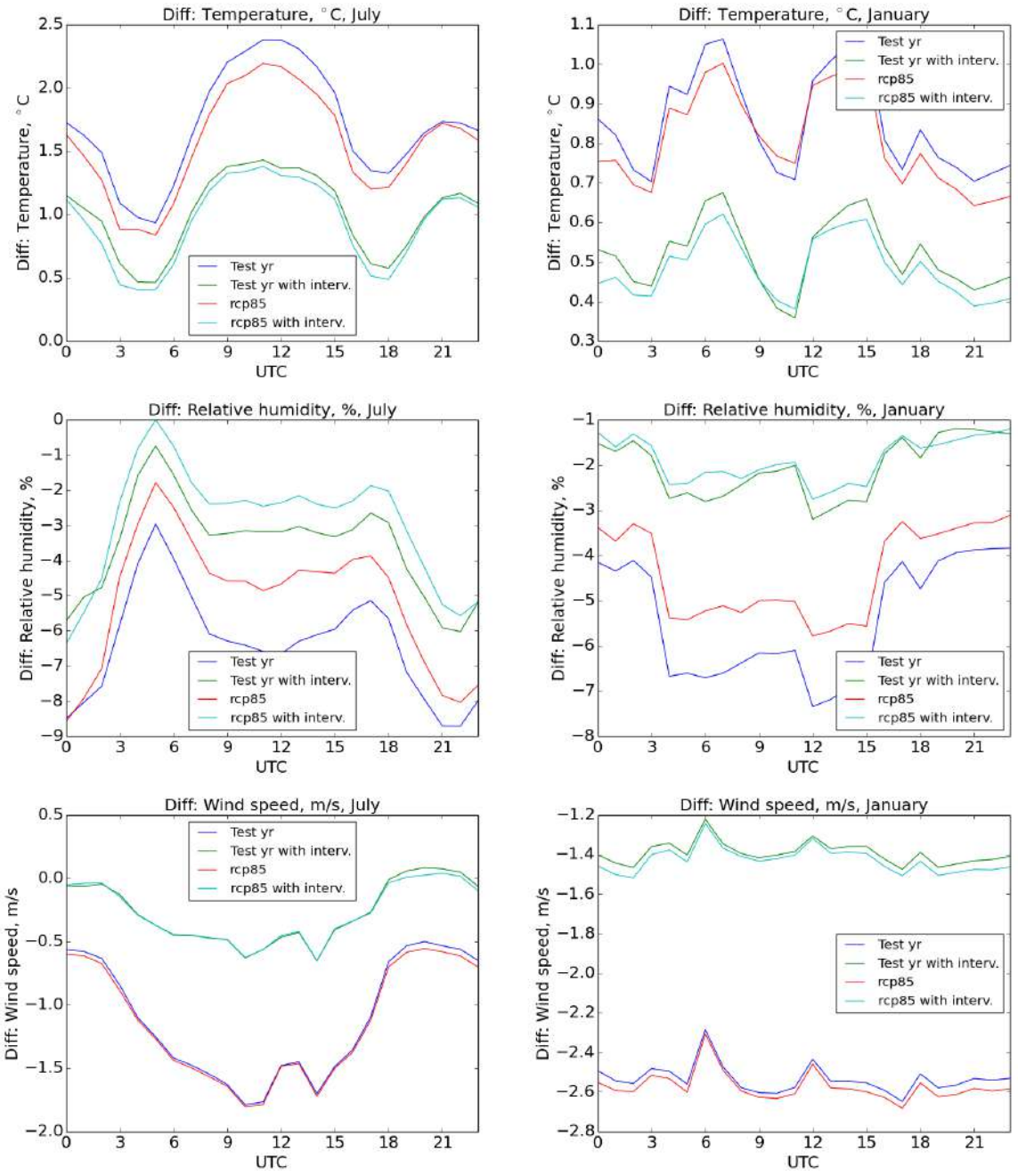

Figure 43: Monthly mean diurnal cycles of difference between Vantaa Tikkurila and the Sipoonkorpi National Park for air temperature (top panels), relative humidity (middle panels) and wind speed (bottom panels), showing the response to changing climate and urban layout in SURFEX for Tikkurila in Vantaa in the months of July (left hand column) and January (right hand column). Local midday occurs at about 10 UTC. Note the different scales on the y-axes

4.6 Summary and discussion of methods and results

The air-surface interaction module SURFEX, with atmospheric forcing obtained from the numerical weather prediction system HARMONIE-AROME, was used to study the climatic influence of the urban and built-up environment within the Helsinki-Vantaa region on the coast of the Gulf of Finland, during an artificially-constructed “test-year” representing the recent past climate of the region and in a future climate corresponding the mid-2050s under the RCP8.5 Representative Concentration Pathway. The HARMONIE-AROME-SURFEX system was validated by comparing results with observations of air temperature, relative humidity, wind speed, and precipitation at the Helsinki-Vantaa airport. The inter-comparison shows the annual and diurnal cycles of temperature, humidity and wind speed to be moderately well reproduced by the model system. Precipitation amount, however, is somewhat underestimated by HARMONIE-AROME during summer, when the precipitation is mainly caused by small-scale scale weather systems such as showers and thunderstorms.

After validation, SURFEX was applied to explore the consequences of altering the urban layout, by replacing relatively densely built commercial and industrial areas with a suburban-type land use featuring lower and less dense buildings and more widespread vegetated areas. For the city of Vantaa, this intervention did not involve any dramatic change in the urban characteristics, and, not unexpectedly, the effect that was seen in the simulations was mainly rather modest, with the exception of wind speeds that increased substantially as a result of the intervention. Based on the present results, we do not expect a major impact on the urban meteorology on spatial scales at and above a city block by altering the urban layout of Vantaa in this way.

However, in the present investigation, a built-up area is treated as a homogenous, isotropic array of street canyons characterized by representative average values of morphological and material parameters describing a grid square of 0.25 square kilometres. The meteorological forcing, in turn, represents an area of about 6.25 square kilometres. Thus, even potentially significant truly local effects of individual structures such as buildings, or stands of trees, are not captured. To investigate such effects, the application of a computational fluid dynamics model resolving the flow field around such structures would be needed.

Comparing results for the test-year and the mid-2050s, it was found that climate warming at street level was only slightly reduced by the simulated changes in urban morphology. For relative humidity and wind speed, by contrast, changes in morphology had an important or even dominating effect, compared with the changing meteorological forcing due to the global warming.

5 Conclusions

The purpose of this Deliverable is to document findings from Task 6.4.1 that focuses on climate projections for all iSCAPE target cities: Bologna in Italy, Bottrop in Germany, Dublin in Ireland, Guilford in United Kingdom, Hasselt in Belgium and Vantaa in Finland. Based on a large number of the CMIP5 global climate model simulations, we have assessed climate change in the six cities around the year 2050. The comprehensive land and ocean surface model SURFEX was used to produce city block-scale meteorological data, taking into account the characteristics of the city-block, the presence and properties of gardens and parks, the radiative and thermal properties of the building materials, as well as anthropogenic sources of heat and moisture from traffic and industry and civil buildings. Specific procedures previously developed by the authors were used together with the CMIP5 model simulation data and the SURFEX model to develop temporally and spatially varying high-resolution scenario weather data for the test case EU City Vantaa. The scenario data account for alternative pathways for mitigation of climate change and evolving urban design and building practices. In summary, this task has produced:

- Local meteorological conditions (currently and in the changing climate) simulated by SURFEX for the test case EU City Vantaa with and without the proposed passive control system (PCS), green infrastructure in this case.
- Validation of SURFEX was based on observations made at the Helsinki-Vantaa airport weather station.
- Climate change projections for the six target cities around the year 2050 under alternative pathways of global greenhouse gas concentrations (RCP4.5 and RCP8.5), considering daily mean, maximum and minimum air temperature, solar radiation, precipitation, air humidity, wind speed and direction.

The main findings regarding future climate change in the iSCAPE cities are:

- The projected changes in the climates of the iSCAPE cities have several common features but also clear differences, particularly so for the annual cycles of the changes.
- Summer is generally the season with largest projected warming, increases in diurnal temperature range and incident solar radiation, and decreases in precipitation. For Vantaa, however, the season with the most pronounced changes is winter.
- Under the RCP8.5 scenario, the projected warming increases almost linearly in time during the course of the ongoing century, most rapidly in Vantaa and slowest in Dublin.
- Apart from Vantaa, the annual mean increases in daily maximum temperature are larger than those in daily minimum temperatures.
- The climatological (30-year average) annual mean precipitation is projected to decrease in Bologna and either increase or remain almost unaltered elsewhere.
- The annual total incident solar radiation is projected increase in all six cities, most strongly in Bottrop and Hasselt and least in Vantaa and Dublin.

Comparing the simulations for the city of Vantaa obtained with and without added green infrastructure, it was found that climate warming at street level was only slightly reduced by the changes in urban morphology. For relative humidity and wind speed, by contrast, changes in morphology had an important or even dominating effect. It should be born in mind, however, that the highly idealized representation of the urban landscape in the SURFEX model cannot resolve

features at scales below that of a city block. Thus, potentially significant local effects of individual structures such as buildings or stands of trees are not captured by the method applied here.

The outcomes of this Task for three iSCAPE cities were previously utilized by WP4 to simulate the interactions of air pollution and climate change, in particular to assess the impact of behavioural changes under future climate scenarios (D4.5 'Report on policy options for AQ and CC'). The output of Task 6.4.1 will form the basis to evaluate the effectiveness of PCSs implementation for air quality and CC in future scenarios (ongoing D6.5). Combined together, the results in D4.5, D6.4 and D6.5 will be utilized in WP7 to derive recommendations on traffic options and infrastructural interventions for the European cities in the present climate and under future climate change scenarios.

6 References / Bibliography

Belcher, S.E., Hacker, J.N., Powell, D.S., 2005. Constructing design weather data for future climates. Build. Serv. Eng. Res. Technol. 26, 49–61.

Bengtsson, L., Andrae, U., Aspelien, T., Batrak, Y., Calvo, J., de Rooy, W., Gleeson, E., Hansen-Sass, B., Homleid, M., Hortal, M., Ivarsson, K.-I., Lenderink, G., Niemelä, S., Nielsen, K.P., Onvlee, J., Rontu, L., Samuelsson, P., Muñoz, D.S., Subias, A., Tijm, S., Toll, V., Yang, X., Køltzow, M.Ø., 2017. The HARMONIE–AROME Model Configuration in the ALADIN–HIRLAM NWP System. Mon. Weather Rev. 145, 1919–1935.

Casanueva, A., Kotlarski, S., Herrera, S. et al. 2016: Daily precipitation statistics in a EURO-CORDEX RCM ensemble: added value of raw and bias-corrected high-resolution simulation. Clim Dyn, 47: 719. https://doi.org/10.1007/s00382-015-2865-x

Christensen, J.H., K. Krishna Kumar, E. Aldrian, S.-I. An, I.F.A. Cavalcanti, M. de Castro, W. Dong, P. Goswami, A. Hall, J.K. Kanyanga, A. Kitoh, J. Kossin, N.-C. Lau, J. Renwick, D.B. Stephenson, S.-P. Xie and T. Zhou, 2013: Climate Phenomena and their Relevance for Future Regional Climate Change. In: Climate Change 2013: The Physical Science Basis. Contribution of Working Group I to the Fifth Assessment Report of the Intergovernmental Panel on Climate Change [Stocker, T.F., D. Qin, G.-K. Plattner, M. Tignor, S.K. Allen, J. Boschung, A. Nauels, Y. Xia, V. Bex and P.M. Midgley (eds.)]. Cambridge University Press, Cambridge, United Kingdom and New York, NY, USA.

Di Sabatino, S., Jylhä, K., Barbano, F., Brunetti, A.F., Drebs, A., Fortelius, C., Nurmi, V., Minguzzi, E., Pulvirenti, B., Votsis, A., 2017. Report on climate change and air quality interactions. iSCAPE Deliverable 1.4 (v 0.5).

Eyring, V., Bony, S., Meehl, G.A., Senior, C.A., Stevens, B., Stouffer, R.J., Taylor, K.E., 2016. Overview of the Coupled Model Intercomparison Project Phase 6 (CMIP6) experimental design and organization. Geosci. Model Dev. 9, 1937–1958.

Gharbia, S.S., Abhijith, K. V., Schmitt, H.C., Gollmann, C., Skouloudis, A.N., Britta, W., Hurth, F., Kirstein, M., Pilla, F., Greiving, S., Kumar, P., 2018. Guidelines to Promote Passive Methods for Improving Urban Air Quality in Climate Change Scenarios. iSCAPE Deliverable 1.2 (v 0.7).

IPCC, 2013. Climate Change 2013: The Physical Science Basis. Contribution of Working Group I to the Fifth Assessment Report of the Intergovernmental Panel on Climate Change. Cambridge University Press, Cambridge, United Kingdom and New York, NY, USA.

Jacob, D., Petersen, J., Eggert, B., Alias, A., Christensen, O.B. et al., 2014: EURO-CORDEX: new high-resolution climate change projections for European impact research. Reg Environ Change, 14: 563-578 https://doi.org/10.1007/s10113-013-0499-2

Jylhä, K., Jokisalo, J., Ruosteenoja, K., Pilli-Sihvola, K., Kalamees, T., Seitola, T., Mäkelä, H.M., Hyvönen, R., Laapas, M., Drebs, A., 2015a. Energy demand for the heating and cooling of residential houses in Finland in a changing climate. Energy Build. 99, 104–116.

Jylhä, K., Kalamees, T., Tietäväinen, H., Ruosteenoja, K., Jokisalo, J., Hyvönen, R., Ilomets, S., Saku, S., Hutila, A., 2011. Rakennusten energialaskennan testivuosi 2012 ja arviot ilmastonmuutoksen vaikutuksista (Test reference year 2012 for building energy demand and impacts of climate change). Finnish Meteorological Institute, Reports, 2011:6, 110 p.

Jylhä, K., Ruosteenoja, K., Jokisalo, J., Pilli-Sihvola, K., Kalamees, T., Mäkelä, H., Hyvönen, R., Drebs, A., 2015b. Hourly test reference weather data in the changing climate of Finland for building energy simulations. Data Br. 4, 162–169.

Kalamees, T., Jylhä, K., Tietäväinen, H., Jokisalo, J., Ilomets, S., Hyvönen, R., Saku, S., 2012. Development of weighting factors for climate variables for selecting the energy reference year according to the en ISO 15927-4 standard. Energy Build. 47, 53–60.

Lehtonen, I and Jylhä, K., 2019: Tendency towards a more extreme precipitation climate in the Coupled Model Intercomparison Project Phase 5 models. Atmospheric Science Letters, 20, DOI: 10.1002/asl.895, https://rmets.onlinelibrary.wiley.com/doi/full/10.1002/asl.895.

Lehtonen, I., Ruosteenoja, K., Venäläinen, A., Gregow, H., 2014. The projected 21st century forest-fire risk in Finland under different greenhouse gas scenarios. Boreal Environ. Res. 19, 127–139.

Lemonsu, A., Grimmond, C.S.B., Masson, V., 2004. Modeling the Surface Energy Balance of the Core of an Old Mediterranean City: Marseille. J. Appl. Meteorol. 43, 312–327.

Masson, V., 2000. A physically-based scheme for the urban energy budget in atmospheric models. Boundary-Layer Meteorol. 94, 357–397.

Masson, V., Le Moigne, P., Martin, E., Faroux, S., Alias, A., Alkama, R., Belamari, S., Barbu, A., Boone, A., Bouyssel, F., Brousseau, P., Brun, E., Calvet, J.C., Carrer, D., Decharme, B., Delire, C., Donier, S., Essaouini, K., Gibelin, A.L., Giordani, H., Habets, F., Jidane, M., Kerdraon, G., Kourzeneva, E., Lafaysse, M., Lafont, S., Lebeaupin Brossier, C., Lemonsu, A., Mahfouf, J.F., Marguinaud, P., Mokhtari, M., Morin, S., Pigeon, G., Salgado, R., Seity, Y., Taillefer, F., Tanguy, G., Tulet, P., Vincendon, B., Vionnet, V., Voldoire, A., 2013. The SURFEXv7.2 land and ocean surface platform for coupled or offline simulation of earth surface variables and fluxes. Geosci. Model Dev. 6, 929–960.

Räisänen, J., Räty, O., 2013. Projections of daily mean temperature variability in the future: Cross-validation tests with ENSEMBLES regional climate simulations. Clim. Dyn. 41, 1553–1568.

Ruosteenoja, K., Jylhä, K., Kämäräinen, M., 2016. Climate projections for Finland under the RCP forcing scenarios. Geophysica 51, 17–50.

Ruosteenoja, K., Markkanen, T., Venäläinen, A., Räisänen, P. Peltola, H. 2018: Seasonal soil moisture and drought occurrence in Europe in CMIP5 projections for the 21st century. Clim Dyn, 50: 1177 . 1177-1192. https://doi.org/10.1007/s00382-017-3671-4.

Saranko, O., 2019. Modelling winter conditions of streets and pavements in a changing climate. Master's thesis, University of Jyväskylä, Department of Physics.

Taylor, K.E., Stouffer, R.J., Meehl, G.A., 2012. An overview of CMIP5 and the experiment design. Bull. Am. Meteorol. Soc. 93, 485–498.

van Vuuren, D.P., Edmonds, J., Kainuma, M., Riahi, K., Thomson, A., Hibbard, K., Hurtt, G.C., Kram, T., Krey, V., Lamarque, J.F., Masui, T., Meinshausen, M., Nakicenovic, N., Smith, S.J., Rose, S.K., 2011. The representative concentration pathways: An overview. Clim. Change 109, 5–31.